STRUCTURE-FUNCTION ANALYSIS OF THE NON-HELICASE DOMAIN OF *SGS1*, THE BLOOM SYNDROME ORTHOLOG FROM *Saccharomyces cerevisiae*

by

LYNDA TUBERTY-VAUGHAN

A Thesis submitted to the

Graduate School-New Brunswick

Rutgers, The State University of New Jersey

and

The Graduate School of Biomedical Sciences

University of Medicine and Dentistry of New Jersey

in partial fulfillment of the requirements

for the degree of

Master of Science

Graduate Program in Cell and Developmental Biology

written under the direction of

Dr. Steven J. Brill

and approved by

_____

_____

_____

New Brunswick, New Jersey

May, 2011

ABSTRACT OF THE THESIS

Structure-Function analysis of the non-helicase domain of Sgs1, the Bloom Syndrome ortholog from *Saccharomyces cerevisiae*

by LYNDA TUBERTY-VAUGHAN

Thesis Director:

Dr. Steven J. Brill

Bloom's Syndrome (BS) is a rare human disease characterized by genome instability and cancer predispostion. The gene mutated in BS, *BLM*, encodes a member of the RecQ family of DNA helicases. BLM is unique among this family because it is the only RecQ member conserved in unicellular eukaryotes.

Apart from the DNA helicase domain, *BLM/SGS1* orthologs contain a poorly characterized N-terminal domain of about 650 amino acids (aa). In yeast, this domain (Sgs1 1-652) is known to be physiologically important although it's only known roles are to bind Top3 and Rmi1 through its N-terminal 100 aa, and *in vitro* single-strand DNA (ssDNA) binding, ssDNA annealing and strand exchange (SE) activities, through its SE domain (Sgs1 103-323)

My research consisted of structure/function analyses of Sgs1 in its poorly characterized N-terminus of aa 323-652 and I found a domain that is important to Sgs1's function. I interrogated this region by doing systematic deletions and tested these *sgs1* mutants for complementation of synthetic lethality. The allele with the smallest deletion that did not complement *sgs1slx4* synthetic lethality was found to be *sgs1-Δ386-621,* and the allele with the smallest deletion that did not complement *sgs1slx5*, was found to be *sgs1-Δ500-621.* I found that *sgs1-Δ386-621* is physiologically important also through the Top3 slow growth assay.

Furthermore I believe that the difference in results between *sgs1slx4* and *sgs1slx5* will prove significant and warrants further investigation.

I also used a *BLM/GCN4* chimera where the SE domain was replaced with the coiled coil GCN4, and again tested alleles with systematic deletions within aa 323-652 in synthetic lethality assay. I found the smallest essential domain to be *sgs1/gcn4-*Δ*500-621* in the *sgs1slx4* background, and interestingly the same deletion in *sgs1-*Δ*500-621* did grow weakly and complemented synthetic lethality. Therefore I postulate there is some interaction between the SE domain and aa 500-621 that could be physiologically important and again warrants further investigation.

Acknowledgement

I would like to thank my advisor, Professor Steven Brill, for giving me the opportunity to conduct research in his laboratory. Through the advice, instruction and knowledge passed on to me, I have developed substantially as a scientist. I would also like to thank Jan Mullen, Chi Fu Chen and Pragati Sharma, the other members of the lab, for their invaluable input and help.

There have also been many professors who have helped and inspired me during my search for a new career during the last 3 years, too many to name, but no less important to my development.

I appreciate the time and effort expended by my committee members, Professors Andrew Vershon and Kim McKim, and thank them for agreeing to serve.

I would like to thank Ranveig Nordhagen, who 24 years ago gave me a job in Oslo Norway, to work in her lab. This experience inspired my return to science after 20 years of occupations completely different from science.

Lastly, I have to thank all the people in my life who have championed my goal to change careers and start again, I would not be here if it were not for their constant encouragement, support, patience and help. My family: Damon Vaughan, Alice and Emma Tuberty-Vaughan. My parents: John and Dagrunn Tuberty. My mentors: Peter and Dina Engler. My friends: Christine Fairchild, Alexey and John Hennessey, Sarah Bayley, Jennifer Van Vort, Rebecca Noerr, Aileen D'Atri, Patti O'Byrne, Maria Prieto, Holly Sylvestri, YMCA friends, many other kind people and lastly my car pool buddies who gave me the extra time to study instead of driving my teenagers around.

Dedication

I dedicate this thesis to my husband, Damon Vaughan

Table of Contents

List of Tables

List of Figures

INTRODUCTION

Helicases

Helicases are involved in many aspects of DNA metabolism. They are enzymes that move along a nucleic acid substrate and separate double strands using the energy released from Adenosine Triphosphate (ATP) hydrolysis. They can unwind DNA or RNA duplex substrates and are part of many processes that involve nucleic acids including DNA replication, DNA repair, transcription, translation, ribosome synthesis, RNA maturation and RNA splicing and nuclear export processes (Singletone et al. 2007). Helicases are a subgroup of translocases as they are able to move directionally along nucleic acid strands.

The biochemical properties of helicases can be divided into 5 parts: rate, directionality, processivity, step size and active versus passive. Rate defines how many base pairs per second the protein moves. This rate varies from a few base pairs to several thousand base pairs per second and is controlled in different ways but mostly through control of its ATPase rate. Directionality of the helicase is the direction it moves on a single strand in either a 5' to 3' or a 3' to 5' direction. Helicases are usually highly processive going through many ATP hydrolysis events before moving on. The Step size refers to how many base pairs the protein moves during one catalytic cycle/ATP hydrolysis. Active versus passive differentiates those enzymes that unwind the duplex ahead of the replication fork (active) as opposed to those that capture unwound strands as a result of thermal fraying of the strands at the replication fork (passive) (Singletone et al. 2007).

Figure 1

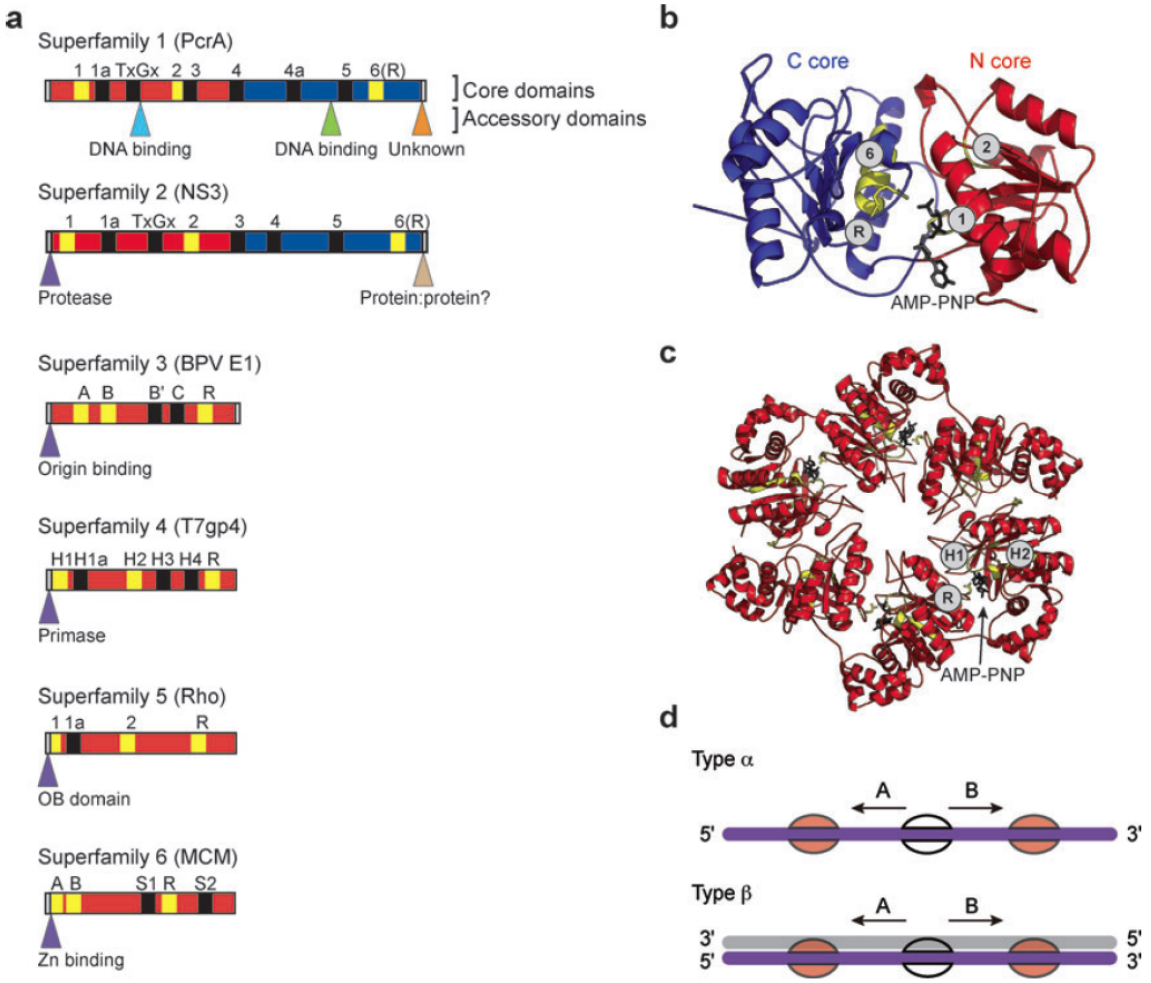
a
Superfamily 1 (PcrA)
1 1a TxGx 2 3 4 4a 5 6(R)
Core domains
Accessory domains
DNA binding
DNA binding
Unknown
Superfamily 2 (NS3)
1 1a TxGx 2 3 4 5 6(R)
Protease
Protein:protein?
Superfamily 3 (BPV E1)
A B B' C R
Origin binding
Superfamily 4 (T7gp4)
H1 H1a H2 H3 H4 R
Primase
Superfamily 5 (Rho)
1 1a 2 R
OB domain
Superfamily 6 (MCM)
A B S1 R S2
Zn binding
b
C core
N core
6
2
R
1
AMP-PNP
c
H1
H2
R
AMP-PNP
d
Type α
A
B
5'
3'
Type β
A
B
3'
5'
5'
3'

Figure 1. Helicase Superfamilies

SF 1-6 with representative members shown in parentheses (a). The "core" domains are based on the example family member and is representative for the whole family. Motifs colored yellow represent universal structural elements in all helicases. Accessory domains in each example protein shown, but are specific to each protein, and their presence, function, and precise location within different members of the same superfamily vary widely. (b, c).Representative core structures. Universal structural elements involved in the binding and hydrolysis of NTP, and the coupling of this activity to conformational changes are shown in yellow. (b).The SF1 and SF2 enzymes contain a monomeric core formed from the tandem repeat of a RecA-like fold. The N- and C-terminal RecA-like domains are shown. An NTP analogue (black) is bound at the interface of the core domains. Motifs 1 and 2, related to the Walker A and B motifs, are located on the N-core side of the cleft. Motif 6, which contains an arginine finger residue, is contributed by the C-core domain. This representative structure is the core of PcrA helicase from SF1. (c) SF3-6 enzymes contain a core that consists of six individual RecA- or AAA+-like domains (red) arranged in a ring. Six nucleotide-binding pockets are present, one at each domain interface, and four are occupied with NTP analogues (black). As in the SF1/SF2 enzymes, conserved elements for the binding and hydrolysis of NTP related to the Walker A and B motifs are located on the opposite side of the cleft compared to the conserved arginine finger residues. This representative structure is of T7 gene 4 protein from SF4. (d).Nomenclature for subfamilies is based on translocation directionality [3'-5' (A) or 5'-3' (B)] and whether the nucleic acid substrate is single (α) or double stranded (β). The strand along which translocation takes place is depicted in purple (Singleton et al. 2007).

Helicases can be divided into six Superfamilies based on the variations of number of motifs, amino acid sequence, and spacing (Fig 1). Superfamilies 1 to 3 (SF1-SF3) are the largest and SF1 and SF2 have at least seven conserved motifs (I, Ia, II, III, IV, V, and VI) and are monomers, whereas SF3–SF5 members assemble into hexamers. The conserved motifs vary across the Superfamiles and there is a universal structural and mechanistic theme across all six. They all posses 'core domains' that form tandem RecA-like folds either within the same polypeptide chain or between subuits. These convert chemical to mechanical energy by coupling NTP binding and hydrolysis to protein conformational changes. Another universal feature of the core domains include conserved residues involved in the binding and hydrolysis of the NTP equivalent to the Walker A (phosphate-binding loop, or p-loop) and Walker B (Mg^{2+}-binding aspartic acid) boxes of many ATPases. For the SF1/SF2 helicases, a single polypeptide chain contains two RecA- like folds. The other Superfamilies are hexameric (or double-hexameric) rings formed from 6 (or 12) individual RecA folds (reviewed in ref Singletone et al. 2007).

Superfamily1 (SF1) helicases are the best-characterized class from a structural perspective, UvrD being one member. UvrD is an E.coli gram negative helicase (3' to 5' directionality) involved in DNA repair. Base–base mismatches can occur as errors of DNA polymerases. The mismatch repair (MMR) process in E. coli involves recognition of the error by a MutS homodimer, which recruits a homodimer of MutL. MutS-MutL activates MutH, which incises the strand. UvrD helicase unwinds the ends of the nicked error-containing strand, followed by exonuclease-mediated digestion. The resulting gap is filled by RNA polymerase III followed by sealing the remaining nick by DNA ligase

The SF2 enzymes are the largest Superfamily and are implicated in diverse cellular processes. They include several heavily studied subfamilies, including DEAD-box RNA helicases and the RecQ-like family (which will be discussed in detail later). Eukaryotic initiation factor-4A (EIF4A), was one of the first DEAD-box RNA helicases to be structurally and biochemically characterized. EIF4A is involved in translation initiation as part of the cap-binding complex. The role of EIF4A is to unwind RNA secondary structure in the 5' UTR of mRNA to facilitate ribosome binding

The SF3 helicases were originally identified in the genomes of small DNA and RNA viruses. SF3 proteins share four conserved motifs, A, B, B', and C. The A and B motifs correspond to the canonical Walker A and B boxes, whereas motif C is SF3 specific (reviewed in ref Singletone et al. 2007). In conjunction with origin-binding domains, SF3 helicases are responsible for distorting DNA before replication forks can be assembled. At these forks, the SF3 helicases act as replicative helicases. The simian virus 40 is a member of SF3 helicases and forms a hexameric ring, anticipated to be characteristic of the entire Superfamily and has a 3' to 5' translocation directionality (Hickman et al 2005).

Members of SF4 were first identified in bacteria and bacteriophages and act as replicative helicases. In bacteria, the helicase associates with a primase, and the two proteins are separate polypeptides (e.g., E.coli DnaB and DnaG proteins), whereas in some bacteriophage systems, both activities reside within a single polypeptide. All characterized SF4 helicases have 5′-3′ (type B) polarity. There are five sequence motifs that define SF4: H1, H1a, H2, H3, and H4 (reviewed in ref Singletone et al. 2007). DnaB is a member of SF4 and is a ring-shaped, hexameric helicase that unwinds the E.coli DNA replication fork while encircling one DNA strand. DnaB can also encircle both DNA strands and then actively translocate along the duplex. With two strands

positioned inside its central channel, DnaB translocates with sufficient force to displace proteins tightly bound to DNA with no resultant DNA unwinding. Thus, DnaB may clear proteins from chromosomal DNA. Furthermore, while encircling two DNA strands, DnaB can drive branch migration of a synthetic Holliday junction with heterologous duplex arms, suggesting that DnaB may be directly involved in DNA recombination in vivo. DnaB binds to just one DNA strand during branch migration (Kaplan et al 2002). T7 phage gp4 protein also drives DNA branch migration, suggesting this activity generalizes to other ring-shaped helicases

Although the Rho helicase is closely related to the SF4 enzymes, it was placed in a separate family (SF5) on the basis of its sequence. Rho is responsible for the termination of transcription in bacteria by binding to a specific sequence on the nascent RNA and then unwinding the DNA/RNA hybrid. Binding activates the RNA-dependent ATPase activity of Rho, which drives the movement of Rho hexamer along the RNA transcript in a 5' to 3'direction.

The last Superfamily, SF6, has as its defining feature the structure of AAA+ proteins which is a structurally conserved ATP- binding module that oligomerizes into active arrays. ATP binding and hydrolysis events at the interface of neighboring subunits drive conformational changes within the AAA+ assembly that direct translocation or remodeling of target substrates (Erzberger et al. 2006). One member of this family is Mini Chromosome Maintenance complex (MCM), a large replication fork eukaryotes helicase complex that is composed of Mcm2-7, Cdc45, and GINS. The Mcm2-7 proteins form a heterohexameric ring that hydrolyzes ATP and provides the motor function for this unwinding complex that has a 3' to 5' polarity.

RecQ Helicase Family

RecQ-like DNA helicases, named after the DNA repair protein RecQ of Escherichia coli are evolutionarily highly conserved from bacteria to humans and are a member of Superfamily 2 (SF2) of DNA helicases (Fig. 2). They perform functions in the maintenance of genome stability and their mutations are associated with cancer predisposition and premature aging syndromes in humans. Most unicellular organisms express a single RecQ family member, whereas multicellular organisms express two or more (Fig. 2). Human cells contain five RecQ proteins named *RECQ1, BLM, WRN, RECQ4* and *RECQ5*.

Figure 2

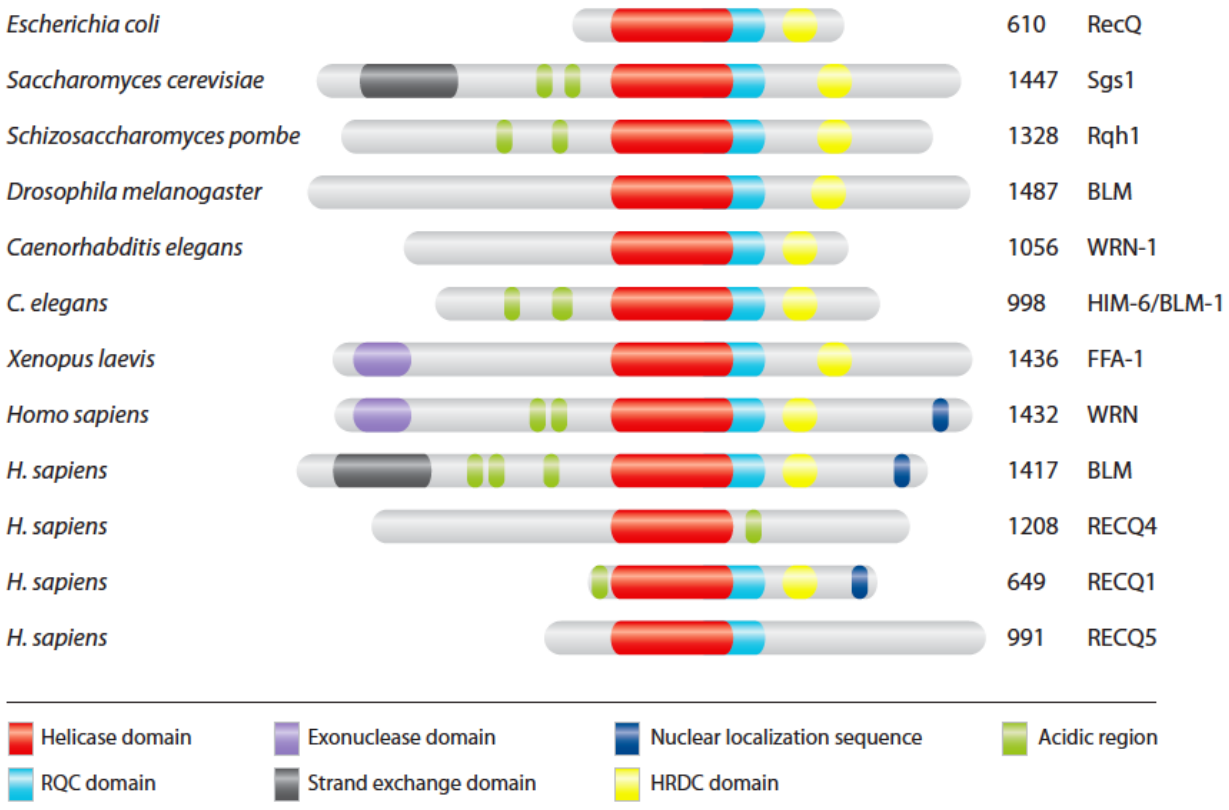

Figure 2 Structural features of RecQ helicases*. The RecQ proteins have several structural domains that are conserved from bacteria to humans. All RecQ proteins have a core helicase domain. Most RecQ proteins also contain conserved helicase and RNAse D C-terminal (HRDC) and RecQ C-terminal (RQC) domains. Many RecQ proteins have acidic regions that enable protein-protein interactions, and some of the RecQ proteins have nuclear localization sequences. WRN and FFA-1 protein contain an exonuclease domain. Sgs1 and Blm are the first characterized members of this family of proteins containing a functional strand exchange domain in their N-terminus. The number of amino acids in each protein is indicated on the right (Bernstein et al. 2010).*

In humans, mutations in *BLM*, *WRN*, or *RECQ4* lead to separate genetic diseases, Bloom, Werner, and Rothmund-Thomson syndromes, respectively (Table 1). Bloom syndrome is a rare autosomal recessive genetic disorder characterized by growth retardation, light sensitivity, immunodeficiency, male infertility, and increased cancer (Seki et al 2008) (Table 1). The predisposition of Bloom patients to develop all types of cancers, frequently occurring by the fourth decade of life, is the primary cause of death and correlates with chromosomal breaks and Sister-chromatid exchange (SCE). Werner syndrome leads to premature aging, with an early onset of diseases like cataracts and osteoporosis, as well as genomic instability predisposing these patients to tumor formation (Seki et al 2008) (Table 1). Cells derived from Werner patients show an increased frequency of chromosomal rearrangements such as translocations, inversions, and deletions. Werner patients' tumors are distinct from those of Bloom patients, being mainly of mesenchymal origin, such as sarcomas (Huang et al 2006). Mutations in *RECQ4* are associated with three unrelated disorders; Rothmund-Thomson syndrome (RTS), RAPADILINO syndrome, and Baller-Gerold syndrome (BGS). All of these disorders are characterized by growth retardation and radial defects. However, RAPADILINO syndrome patients do not exhibit poikiloderma, which is characteristic of both RTS and BGS. RTS is the best characterized of the

RECQ4 diseases, and these patients also have skeletal abnormalities, skin disorders, light sensitivity, and age prematurely. Rothmund- Thomson patients are especially susceptible to developing bone and skin cancer, and their cells display increased chromosomal rearrangements like translocations and deletions (reviewed in Bernstein et al. 2010).

Table 1 Clinical Features of RecQ disorders

Syndrome (gene)	Main clinical features	Cancer predisposition
Bloom syndrome (BLM)	Dwarfism, beaked nose, narrow face, pigmentation, redness, and dilated blood vessels in skin, mental retardation, type-II diabetes, immunodeficiency, lung problems, low or no fertility	Early onset with normal distribution of tissue and type
Werner syndrome (WRN)	Bilateral cataracts, hoarseness, skin alterations, thin limbs, premature gray/loss of hair, pinched facial features, short stature, osteoporosis, hypogonadism, diabetes, soft tissue calcification	Early onset of primary sarcomas and mesenchymal tumors
Rothmund-Thomson syndrome (RECQ4)	Poikiloderma, juvenile cataracts, growth retardation, skeletal dysplasia, sparse scalp hair, hypogonadism	Early onset of osteosarcomas
RAPADILINO syndrome (RECQ4)	Growth retardation, bone malformation in limbs, radial defects such as hypoplasia and aplasia of thumbs and radius, cleft or highly arched palate	Lymphoma and osteosarcoma
Baller-Gerold syndrome (RECQ4)	Craniosynostosis, radial aplasia and hypoplasia, poikiloderma, growth retardation	Not applicable

(Bernstein et al. 2010)

RecQ helicases share key functional domains that are conserved in most bacterial and eukaryotic RecQ proteins by sequence analysis. (Fig 2). All RecQ-like helicases share a seven-motif helicase domain with Walker A and DEAH box, which functions to unwind dsDNA in an ATP and Mg^{2+} dependent manner and travel on single-stranded DNA (ssDNA) in a 3' to 5' direction. The unwinding activities of helicases are coordinated by seven sequence motifs plus a motif 0 that is N-terminal to motif I that is specific to RecQ helicases. A mutation of the conserved motif 0 glutamine to arginine is sufficient to cause Bloom Syndrome (BS) and abolishes its ATPase and DNA-unwinding activities (Bahr, De Graeve et al. 1998; German, Sanz et al. 2007). The mutations of the invariant phosphate-binding lysine residue in motif I in *BLM*

and the yeast Sgs1 helicase (Mullen et al. 2000) also seriously impairs' or abolishes their ATPase and DNA-unwinding functions.

The RecQ-helicase-conserved (RQC) domain, located C-terminal to the helicase domain, is considered important for both the structural integrity of the protein and dsDNA binding (Guo at al. 2005, Bennett et al. 2004). It might also have a role in mediating interactions with other proteins (Lee et al. 2005), is thought to be involved in DNA binding and conferring specificity of binding to DNA structures, such as G4 tetrads.(von Kobbe et al. 2003, Huber et al. 2006). The RQC region was first determined to contain a Zn2+-binding domain and a winged helix domain from the crystal structure of E.coli RecQ (Fig. 3).

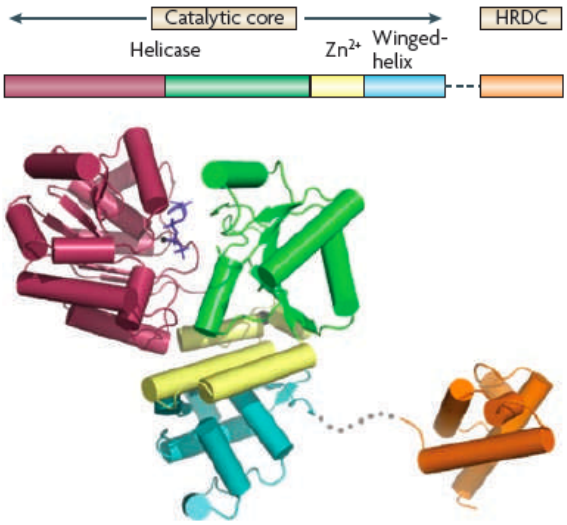

Figure 3. Structure of the Escherichia coli RecQ protein. *Conserved regions are shown at the top in the schematic diagram. Helicase regions are shown in red and green, the Zn2+-binding subdomain in yellow, the winged-helix subdomain in turquoise and the Helicase and RNase D C-terminal (HRDC) domain in orange. The helicase and RecQ carboxy-terminal domains are considered to be the catalytic core of the enzyme. The ribbon diagram of the crystal structure of E. coli RecQ is shown with a bound ATPgammaS molecule (lavender). alpha-helices are shown as cylinders and beta-sheets as arrows. The grey dotted line between the winged-helix and HRDC domains denotes a region for which the structure has not been solved. (Chu et al. 2009)*

The Helicase/ RNase D C-terminal (HRDC) domain is the most C-terminal of the conserved domains and resembles domains in other proteins that are involved in nucleic acid metabolism, such as RNase D and UvrD; however, similar to the RQC domain, it is not found in all RecQ-like helicases. The HRDC domain has been implicated in binding and resolving DNA structures, such as Holliday junctions, and in mediating protein–protein interactions. Two acidic regions have also been identified N-terminal of the helicase domain and may be involved in mediating protein–protein interactions (Bernstein et al 2009). In addition to the helicase, RQC, and HRDC domains, some members possess a 3′ →5′ exonuclease domain in their N terminus (*WRN* and Xenopus laevis FFA-1), a nuclear localization signal in their C terminus (*BLM* and *WRN*) (reviewed in ref Mirzaei et al. 2010). Recently, a new functionally conserved domain mediating strand annealing and strand exchange has been uncovered in the N terminus of Sgs1 and *BLM* (Chen et al. 2010).

SGS1

Bloom's syndrome (BS) is a rare autosomal recessive disorder in humans. It is characterized by small stature, sun sensitivity with facial erythema, infertility in males, reduced fertility in females, a short life span of only 20–30 years, and an increased risk of a wide range of cancers. Cells from BS patients contain mutations in the *BLM* gene, and have an increased level of chromosomal breaks, translocations and sister chromatid exchanges. Therefore, the *BLM* protein is thought to be required for the prevention and/or resolution of aberrant DNA structures that lead to these chromosomal abnormalities (Ashton et al. 2010). The budding yeast Saccharomyces cerevisiae only has one RecQ helicases, *SGS1*, and this is the homolog of *BLM*. *BLM* interacts with the type IA topoisomerase, *hTOPOIII* (Wu et al. 2000), and *hRMI1* (Chen et al. 2007). These interactions are conserved as Sgs1 physically interacts with Top3 and Rmi1 (Fig. 4) (Mullen et al. 2005, Fricke et al. 2001). This has been termed the RecQ helicase-topoisomerase III-Rmi1 (RTR) complex (Mankouri et al. 2007).

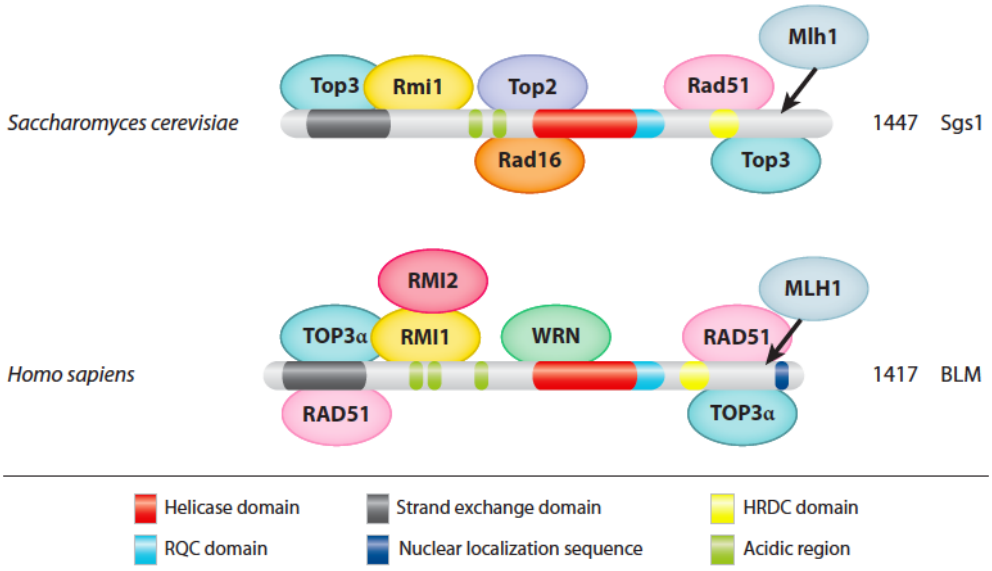

***Figure 4. Conserved interactions between DNA repair and recombination proteins with Sgs1 and* BLM**. *In yeast, Sgs1 physically interacts with many different repair and recombination proteins, such as Top3, Rmi1, Top2, Rad16, Mlh1, and Rad51, shown here as ovals. Many of these interactions are evolutionarily conserved in the human* BLM *protein.* BLM *also interacts with* WRN, *another RecQ helicase, and* RMI1 *interacts with* RMI2. *Arrows show the positions of residues critical for the interactions of each protein with Mlh1/*MLH1. *Although Sgs1 and* BLM *interact with other partners, only those DNA repair/replication proteins whose interaction regions are known are displayed. (Bernstein et al. 2010).*

The failure to repair DNA damage can lead to genomic instability such as those seen in Bloom's Syndrome. The study of the yeast homologue, *SGS1*, has revealed many roles for this protein in repair of double strand breaks, restart of stalled replication forks, and processing of aberrant intermediates that arise during meiotic recombination and maintenance of teleomeres. Many of these roles are accomplished through the important pathway of Homologous Recombination (HR).

Sgs1's multiple roles in repair of double strand breaks by Homologous Recombination.

HR repair involves the transfer of genetic material between two identical or closely homologous DNA sequences. The primary function of the pathway is probably to restart stalled or broken replication forks, but it is also required for the repair of double strand breaks (DSBs) and inter-strand DNA crosslinks. DSBs can be induced by chemicals or irradiation, but can also occur as intermediates of meiotic recombination or yeast mating- type switching. HR repair at a DSB involves degradation of the 5′ terminating DNA strand at either side of the break, a process that is termed resection (Fig. 5) (Bernstein et al. 2009). Resection results in a 3′ ssDNA strand that becomes bound by replication protein A (RPA). RPA is then displaced by Rad51, forming a presynaptic filament that invades the sister chromatid, or the homologous chromosome in diploid cells, to form a displacement loop (D-loop). Once the invading 3′ ssDNA strand identifies the region of sequence homology, DNA synthesis occurs to restore the missing sequence from the invading strand. This strand may then be displaced, allowing repair to be completed by the synthesis-dependent strand annealing (SDSA) subpathway of HR. DNA synthesis can occur to fill the gaps, which are ligated to form a double Holliday junction (DHJ). These DHJs are resolved to complete repair. During the mitotic cell cycle, HR repair operates exclusively in S phase and G2/M, when the sister chromatid can act as a template for repair. It also operates in meiosis, when the homologous chromosome is also able to act as a template. Sgs1 has a role in both the resection and DHJ resolution steps of the HR pathway.

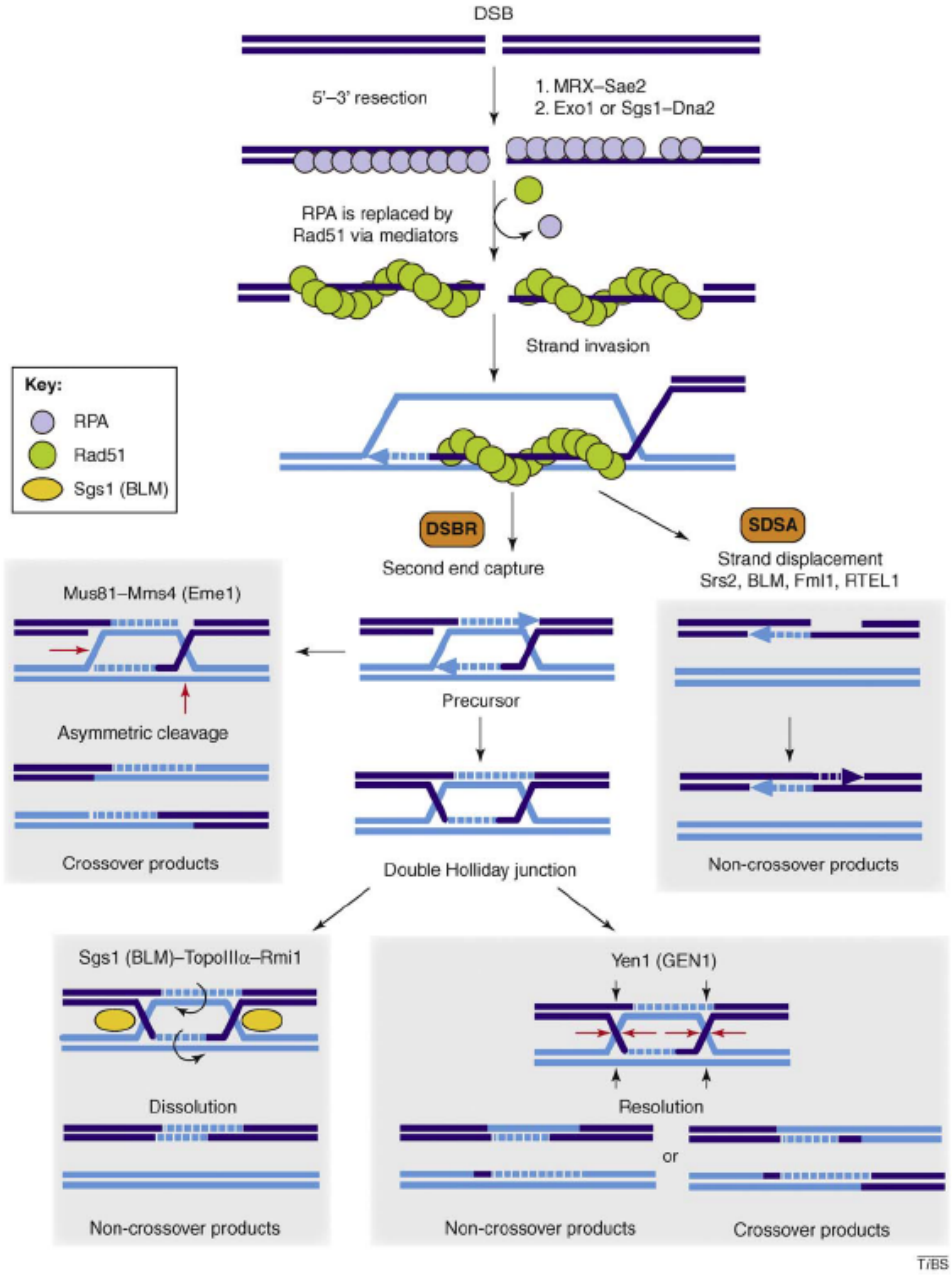

Figure 5. Models and outcomes of the homologous recombination pathway*. 5'–3' resection of the broken ends creates 3' ssDNA tails that are rapidly coated by RPA (light blue). RPA is replaced by Rad51 (green) to form the nucleoprotein filament, which can initiate pairing and strand invasion with the homologous duplex DNA. The 3' end of the invading strand is extended by DNA synthesis using the donor duplex as a template. In the SDSA model, the invading strand is displaced and pairs with the other 3' single stranded tail, allowing DNA synthesis to complete repair. In the DSBR model, second end capture forms an early strand exchange intermediate. Processing of this precursor by Mus81–Mms4 (Eme1) generates crossover products, and ligation of this precursor creates a DHJ. Dissolution of the DHJ (via Sgs1 [*BLM*]–TopoIIIa-Rmi1) gives rise to non-crossover products, whereas resolution (via Yen1 [*GEN1*]) can lead to either crossover or non-crossover products (Mimitou et al. 2009).*

The first step in this pathway that involves Sgs1 is DNA end resection, to generate a 3' single stranded DNA (ssDNA) overhang which becomes a substrate for the DNA strand exchange protein, Rad51. Cejka and colleagues biochemically reconstituted the elements of the resection process and reveal that it requires the nuclease Dna2, the RecQ-family helicase Sgs1 and the ssDNA-binding protein replication protein-A (RPA). They establish that Dna2, Sgs1 and RPA constitute a minimal protein complex capable of DNA resection in vitro. Sgs1 helicase unwinds the DNA to produce an intermediate that is digested by Dna2, and RPA stimulates DNA unwinding by Sgs1. In addition to this core machinery, Cejka and colleagues establish that both the topoisomerase 3 (Top3) and Rmi1 complex and the Mre11–Rad50–Xrs2 complex (MRX) have important roles as stimulatory components. Stimulation of end resection by the Top3–Rmi1 heterodimer and the MRX proteins is by complex formation with Sgs1 (Gangloff et al. 1994, Chiolo et al. 2005) which stimulates DNA unwinding. Cejka and colleagues suggest that Top3–Rmi1 and MRX are important for recruitment of the Sgs1–Dna2 complex to DSBs. (Cejka et al. 2010). Niu and colleagues have shown that DNA strand separation during end resection is mediated by the Sgs1 helicase function, in a manner that is enhanced by Top3-Rmi1 and MRX. (Niu et al. 2010)

The next step in recombinational repair is homology search and strand invasion. The ssDNA is coated with Rad51 and this nucleoprotein filament searches for complementary sequences in dsDNA. During strand invasion and pairing, the noncomplementary strand of the duplex is displaced, creating a D-loop, a process that can occur at collapsed replication forks. In vitro, Rad51 efficiently forms D-loops with either a 5′ or a 3′ invaded end. However, only the 3′ invaded end is proficient for priming new DNA synthesis to allow extension of the D-loop by DNA polymerase. The cross-strand structures formed during this process can also branch

migrate. RecQ helicases including Sgs1 can unwind a variety of DNA substrates with a marked preference for Holliday junction's (HJ), G-quadruplexes and D-loops (Bennett et al. 1999, Cejka et al. 2010, Harmon et al. 1998, Mohaghegh et al. 2001, Sun et al. 1999, Van Brabant et al. 2000).. All biochemical identification of enzymatic activities of Sgs1 have been completed with truncated forms until very recently. Cejke and colleagues were able to express and purify the full-length protein and found that Sgs1 binds diverse single-stranded and double-stranded DNA substrates, including DNA duplexes with 5' and 3' single-stranded DNA overhangs. Similarly, Sgs1 unwinds a variety of DNA substrates, including blunt-ended duplex DNA. Significantly, a substrate containing a HJ is unwound most efficiently. (Cejke et al. 2010). Once the D-loop is formed then SDSA can follow forming a DHJ.

Double Holiday junction migration and dissolution is the next step that involves Sgs1. Once a DHJ has been formed, there are three ways in which it can be resolved to complete the repair (Fig. 5). Each method can produce either crossover or noncrossover recombination products. Endonucleases have been isolated from different species that yield equal numbers of crossover and noncrossover recombination products however crossing over can have deleterious consequences during the mitotic cell cycle by promoting loss of heterozygosity (LOH) between homologous chromosomes. The first method is cleavage by a classical HJ resolvase, which will cut HJs symmetrically on opposing strands to generate products that can be ligated together. The orientation of this cleavage appears to be random, as DHJs resolved by these enzymes likely form 50% crossover where the flanking DNA is exchanged and 50% non-cross-over products (Wu et al. 2003). RuvC from E.coli was the first HJ resolvase to be identified (Dunderdale et al. 1991). More recently Slx1–Slx4 was found to be a nuclear HJ resolvase (Ip et al. 2008, Fricke et al. 2003). The second method of resolving the DHJ intermediate is by the heterodimeric 5′-flap

endonuclease, Mus81–Mms4 in *S. cerevisiae*. (Osman et al. 2007). Purified Mus81–Mms4 complexes from *S. cerevisiae* are able to cleave HJs in vivo, they prefer to cut nicked HJs and D-loops, which suggests that cleavage of intact HJs may be a secondary activity for Mus81–Mms4. Their cleavage of intact HJs is asymmetrical, which produces a mixture of flapped and gapped linear duplexes that must be processed by a flap endonuclease and a gap-filling polymerase, respectively, in order for repair to be completed. The third method for processing a DHJ to complete HR repair is by DHJ dissolution, which is performed by the Sgs1–Top3–Rmi1 (RTR) complex. This is considered the predominant form of DHJ processing as only 5% of recombination events in mitotic cells results in crossovers implying that DNA breaks can be repaired either without DHJ formation or by resolving DHJ without crossing over (Ira et al. 2003, Heyer et al. 2003).

The first unit of the RTR complex to be identified was eukaryotic topoisomerase III (Top3) which is a type I enzyme that it is most active in unlinking single-strand catenanes. Sgs1 interacts genetically and physically with Top3 (Gangloff, et al. 1994, Fricke et al. 2001; Wu et al. 2000). Mutation of *TOP3* results in slow-growth phenotype, high levels of recombination and chromosome loss (Myung et al. 2001, Ui et al. 2005). Slow-growth of *top3* mutants was suppressed by *sgs1*Δ, and yeast two-hybrid data indicated that the Sgs1 N-terminus and Top3 interacted in vivo (Gangloff et al. 1994). Physically interaction studies confirmed that Top3 interacts with the N-terminal 100 aa of Sgs1 (Bennett et al. 2001, Fricke et al. 2001) and is essential for complementation of *sgs1* mutant phenotype (Mullen et al. 2000). Taken together, these results indicate that Sgs1-Top3 functions as a complex and confirm the idea that the *top3* slow-growth phenotype is primarily due to unrestrained Sgs1 DNA helicase activity in the absence of Top3 activity (Gangloff et al. 1994).

sgs1-top3 mutants exhibit DNA damage sensitivity as yeast strains lacking *TOP3* either arrest or delay in G2, suggesting a role in repairing spontaneous S-phase damage (Gangloff et al. 1999). Additional support for a role of Sgs1-Top3 in recombination is provided by genetic suppression studies. Several *sgs1-top3* mutant phenotypes appear to result from toxic recombination intermediates, since they are suppressed in strains that are unable to initiate meitotic or mitotic recombination, as evidenced in the finding that *top3*Δ homozygous diploids are capable of undergoing meiosis as long as recombination is not initiated (Gangloff et al. 1999). Similar to the increase in sister chromatid exchanges seen in Bloom syndrome cells, *sgs1* mutants display an increase in crossover frequency compared to wild-type (wt) cells (Ira et al. 2003). This result suggested that the normal function of Sgs1-Top3 is to resolve recombination intermediates in a pathway leading to noncrossover products (Fig. 5).

As an approach to identify genes in the Sgs1-Top3 pathway, Mullen and colleagues employed a synthetic lethal screen with the synthetic interactor *MUS81* (Mullen et al. 2005). Analysis of synthetic-lethal screen candidate genes revealed that one of them, *RMI1*, encoded a component of the Sgs1-Top3 complex. Chen and colleagues found that a stable Top3 Rmi1 complex can be isolated from yeast cells over-expressing these two subunits. Compared with Top3 alone, this complex displays increased superhelical relaxation activity. The isolated Rmi1 subunit also stimulates Top3 activity in reconstitution experiments. Rmi1 only has weak binding to ssDNA on its own, but it stimulates the ssDNA binding activity of Top3 5-fold. Top3 and Rmi1 also cooperate to bind the Sgs1 N terminus and promote its interaction with ssDNA demonstrating that Top3-Rmi1 functions as a complex. (Chen et al. 2007)

Sgs1 helicase, DNA topoisomerase III (Top3) and Rmi1 (RTR complex) act together to prevent chromosome exchanges (Ira et al. 2003, Chang et al. 2005, Mullen et al. 2005). As a

result of these observations it was thought that that these proteins may be acting to process a DHJ (Wang 2002). Because of the lack of full-length Sgs1 protein direct biochemical analysis had only been performed on the human and *Drosophila melanogaster* homologs of these proteins (Wu et al. 2003, Plank et al. 2006, Wu et al. 2006, Bussen et al. 2007, Raynard et al. 2006, Raynard et al. 2008). However Cejka and colleagues recently purified full-length recombinant Sgs1 and they were therefore able to ask whether the *S. cerevisiae* proteins possess this biochemical capability of processing DHJ's. Although genetic studies of these proteins in yeast could be interpreted to support a role in DHJ dissolution, these proteins could also be acting in an alternate pathway that leads to non-crossovers. To address these questions, they tested these proteins on a mobile, topologically constrained DHJ substrate (DHJS) (Cejka et al. 2010).

Dissolution of a DHJ was initially defined using a model oligonucleotide-based substrate that possessed two junctions separated by two topological links that required little or no branch migration to separate the oligonucleotides (Wu et al. 2003). Cejka and colleagues used a much larger DHJS that recapitulates many of the features of an endogenous DHJ (Plank et al. 2006). It is most easily envisioned as a pair of double-stranded DNA (dsDNA) rings conjoined by two HJs, with 165 base pairs (bp) of homologous dsDNA between each junction (Fig. 6). The homology between the two HJs allows for the convergent migration of the HJs without the obligate generation of large tracts of single-stranded DNA (ssDNA), and the dissolution of this substrate requires both branch migration and DNA strand passage to separate the conjoined DNA molecules. Owing to the distance between the two HJs, 30–35 strand passage events are required to separate the two DNA rings, providing a rigorous test for proteins thought to participate in DHJ dissolution.

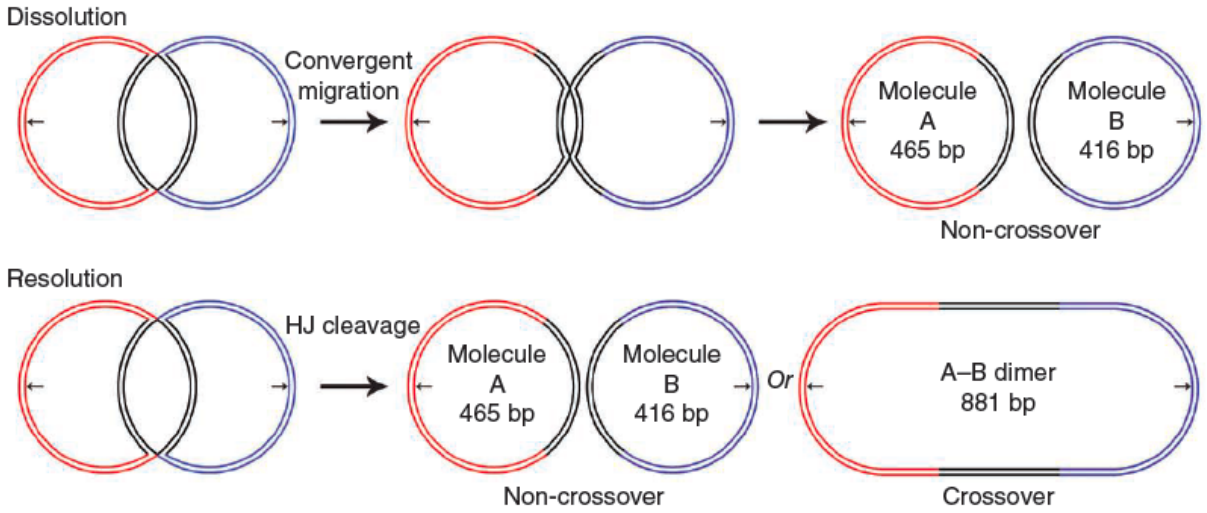

***Figure 6**.A schematic representation of the DHJ substrate (DHJS). Top, dissolution of the DHJS by convergent branch migration leads exclusively to monomeric non-crossover products (A and B). Bottom, resolution by nucleolytic cleavage leads to either monomeric non-crossover products (A and B) or a dimeric crossover product (A–B dimer). Small arrows indicate BamHI restriction sites.(Cejka et al. 2010)*

Cejka and colleagues report that *S. cerevisiae* Sgs1 and Top3 are capable of dissolving the DHJS in a reaction that is largely species specific (if Sgs1 was replaced by hBLM, EcRecQ or Srs2, the dissolution reaction did not complete to 100% non-crossover products and only resulted in a convergently branch migrated intermediary and the original DHJ), implying that specific protein-protein interactions are important for this activity. At low protein concentrations, Rmi1 stimulates dissolution of the DHJS, although it does not stimulate the rate of convergent branch migration of the HJs. Further studies using an oligonucleotide-based DHJ substrate confirmed that Rmi1 more strongly stimulated the dissolution reaction when the two HJs were in close proximity. They go on to show that Rmi1 stimulates the decatenation activity of Sgs1–Top3 and is likely stimulating the dissolution reaction at the final decatenation step. These results confirm that DHJ dissolution is an evolutionarily conserved process, and they define a previously unknown role for Rmi1 in this pathway of stimulating decatenation. (Cejka et al. 2010)

Sgs1 might have an anti-recombinogenic role to prevent the use of inappropriate templates for HR, such as homeologous sequences and aberrant break-induced replication intermediates. The strand exchange domain (SE) shows ssDNA annealing and strand exhchange activities that is inhibited by a single mismatched base repair (Chen et al. 2010). Sgs1 is also able to suppress repair by single-strand annealing at a DSB flanked by 205bp homeologous sequences (Sugawara et al. 2004, Myung et al. 2001). The rate of GCRs is increased in *sgs1*Δ mutants also suggesting an anti-recombinogenic role in suppression of gross chromosomal rearrangements (Myung et al. 2001).

Repair of replicative damage and restart of stalled replication forks.

During DNA replication, the RecQ helicases help enable the association of the polymerases with the replication fork, unwind DNA structures that potentially lead to replication fork stalling (i.e., G-quadruplexes and hairpin structures), and resolve hemicatenane-like structures that can form during repair of replicative damage. Replication forks can stall if nucleotide production is compromised, or when the replisome encounters secondary structures in the template or obstructive DNA lesions. Well-studied agents that are known to cause fork stalling include methyl methanesulphonate (MMS), and hydroxyurea (HU). MMS is an alkylating agent that methylates DNA on N^7-deoxyguanine and N^3-deoxyadenine, the latter of which blocks progression of DNA polymerases. HU is an inhibitor of ribonucleotide reductase, which catalyses dNTP production (Ashton et al. 2010). Once a fork has stalled, the intra-S phase checkpoint is activated, functioning to suppress late origin firing, to stabilize the stalled fork and to recruit of proteins to the fork for its repair and restart. Recruitment of Sgs1 to replication forks stalled by HU is required for the activation of the DNA damage checkpoint kinase, Rad53 (Bjergbaek et al. 2005). Sgs1 binds to Rad53 in vitro and in vivo, and these proteins colocalise in S phase specific nuclear foci (Bjergbaek et al. 2005, Frei et al. 2000). The helicase activity of Sgs1 is dispensable for the activation of Rad53, and therefore is likely to be mediated via the physical interaction between Sgs1 and Rad53. The activation of Rad53 may be the only role of Sgs1 at forks stalled by HU, as HR intermediates are not detected by 2D gel electrophoresis in *sgs1*Δ cells treated with HU (Liberi et al. 2005). HR intermediates do accumulate in MMS treated *sgs1*Δ cells therefore Sgs1 must have multiple roles at MMS-stalled forks (Liberi et al. 2005, Mankouri et al. 2007, Mankouri et al. 2006). Top3 and Rmi1 are not required for activation of Rad53 at HU-stalled forks, but are involved in Rad53 activation MMS-stalled forks, as Rad53 is not fully activated in MMS-treated *top3*Δ and *rmi1*Δ mutants (Chang et al.2005,

Chakraverty et al. 2001). This Rad53 activation does not require Top3 catalytic activity, so may be mediated via protein–protein interactions, perhaps through Sgs1 (Mankouri et al. 2006). Sgs1 is found in chromatin Immunoprecipitation (ChIP) experiments at unperturbed replication forks. Furthermore, using HU or MMS to stall or collapse the replication fork contributed to polymerases' ability to efficiently immunoprecipitate with the replication fork (Cobb et al. 2003). When replication fork damage is induced with MMS, X-shaped molecules form at replication origins, which are revealed by two-dimensional gel electrophoresis. These X-structures likely contain ssDNA because their formation is sensitive to Mung Bean nuclease (Liberi et al.2005). Complete disruption of *SGS1* or a point mutation in its helicase domain leads to the accumulation of these X structures at damaged forks (Bernstein et al. 2009, Liberi et al. 2005). It is possible to isolate mutants of *SGS1* that encode proteins defective in repair of replicative damage but do not influence recombination at other loci, indicating that the function of Sgs1 in repair of replicative damage is distinct from its function in resolution of HR intermediates (Bernstein et al. 2009). Sgs1 has also been found to bind to forked DNA substrates in vitro (Bennet et al. 1999, Cobb et al. 2003). Taken together it has been implied that the RTR complex is involved in the repair and restart of stalled forks (Ashton et al. 2010).

Sgs1's functions during meiosis and teleomere maintenance.

Meiotic recombination generates genetic diversity. The process of homologous recombination during meiosis is necessary for ensuring accurate chromosome segregation. Sgs1 was implicated as being involved in meiotic recombination as s*gs1*Δ mutants exhibit reduced tetrad formation and spore viability (Gangloff et al. 1999). Homologous recombination during meiosis is initiated by a DSB catalysed by Spo11. Following the formation of the DSB, 5' strand resection generates 3' single-stranded overhangs that are then able to invade the homolog. Strand

invasion is facilitated by the strand-exchange proteins Rad51 and Dmc1 and leads to the formation of a Single End Invasion (SEI) structure. These breaks are then repaired either through the crossover pathway involving resolution of the DHJ junction formed, or non-crossover pathway involving SDSA and dissolution of the DHJ as discussed earlier. When Sgs1 is deleted there is an increase in meiotic recombination between diverged sequences (homeologous recombination) and an increase in unequal sister chromatid events. Sgs1 is involved in the rejection of 'second strand capture' when sequence divergence is present (Amin et al. 2010). This is also supported by the ability of the SE's domain to anneal to both homologous and homeologous DNA, but its divergent ability to strand exchange (SE) homologous DNA but not homeologous DNA (Chen et al. 2010). Sgs1 also prevents aberrant meiotic crossing over by suppressing the formation of large joint molecules comprising three or four interconnected DNA duplexes (Oh et al. 2007). In meiosis, interhomologue crossing over is promoted, at the expense of the normally favored recombination between sister chromatids seen in mitotic cells. Sgs1 contributes to this bias in meiosis by reducing the formation of intersister DHJs and favouring the generation of interhomologue DHJs (Oh et al. 2007)

To protect chromosome ends from exonucleolytic degradation, aberrant recombination events, and fusion with other chromosomes, telomeres are regions of repetitive sequences of DNA located at the chromosome ends. Maintenance of telomere length is achieved either by telomerase, or by an alternative lengthening of telomeres (ALT) pathway, which relies on the proteins involved in HR including Sgs1 (Huang et al. 2001). The ALT pathway permits shortened telomere sequences to invade other telomere sequences, which then serve as a template for telomere extension by conventional DNA polymerases (Cesare et al. 2008).

The uncharacterized N-Terminal region of Sgs1

Apart from the DNA helicase domain, *BLM/SGS1* orthologs contain a poorly characterized N-terminal domain of about 650 amino acids (aa) (Fig. 7a). There is lack of sequence conservation between orthologs of the N-terminus and as a result this has hindered its functional analysis (Fig. 7b). In yeast, this domain (Sgs1 1-652) is known to be physiologically important (Mullen et al. 2000) although it's only known roles are to bind Top3 and Rmi1 through its N-terminal 100 aa, and *in vitro* single-strand DNA (ssDNA) binding, ssDNA annealing and strand exchange (SE) activities, through its SE domain (Sgs1 103-323).

The domain of Sgs1 aa323- 622 remains largely uncharacterized and my objective was to determine a function for this region through systematic interrogation. There are many structure/function analyses that have been performed in this area and following is a summary of current published research. However, the synthetic lethality assay was chosen, as this assay had not been used to examine this region previously.

Figure 7. Clustal W alignment of BLM orthologs *was performed using default parameters (http://www.ebi.ac.uk/Tools/clustalw2/index.html). Note that highlighting identifies similar residues. Sequence names include the aa residues used in the alignment: Hs, human; Dr, Danio rerio; Ol, Oryzias latipes; Xl, Xenopus laevis, Gg, Gallus gallus; Dm, Drosophila melanogaster; Kl, Kluvermyces lactis; Sc, Saccharomyces cerevisiae. (**a**)RecQ domains. (**b**) N-terminal domains. The BDHCT region is underlined and spans amino acid 371-411 of* Sgs1.

Figure 7 (a)

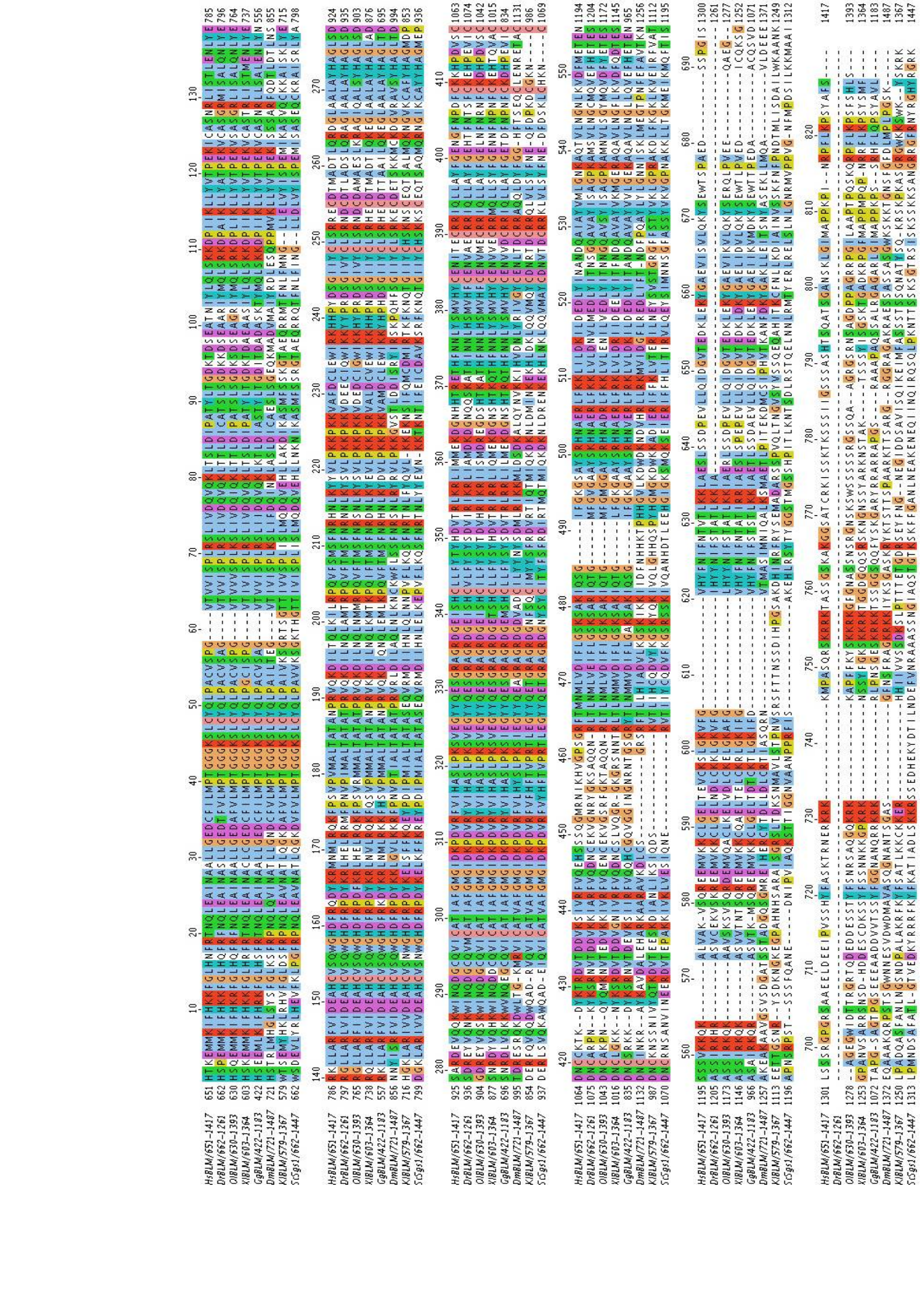

Figure 7 (b)

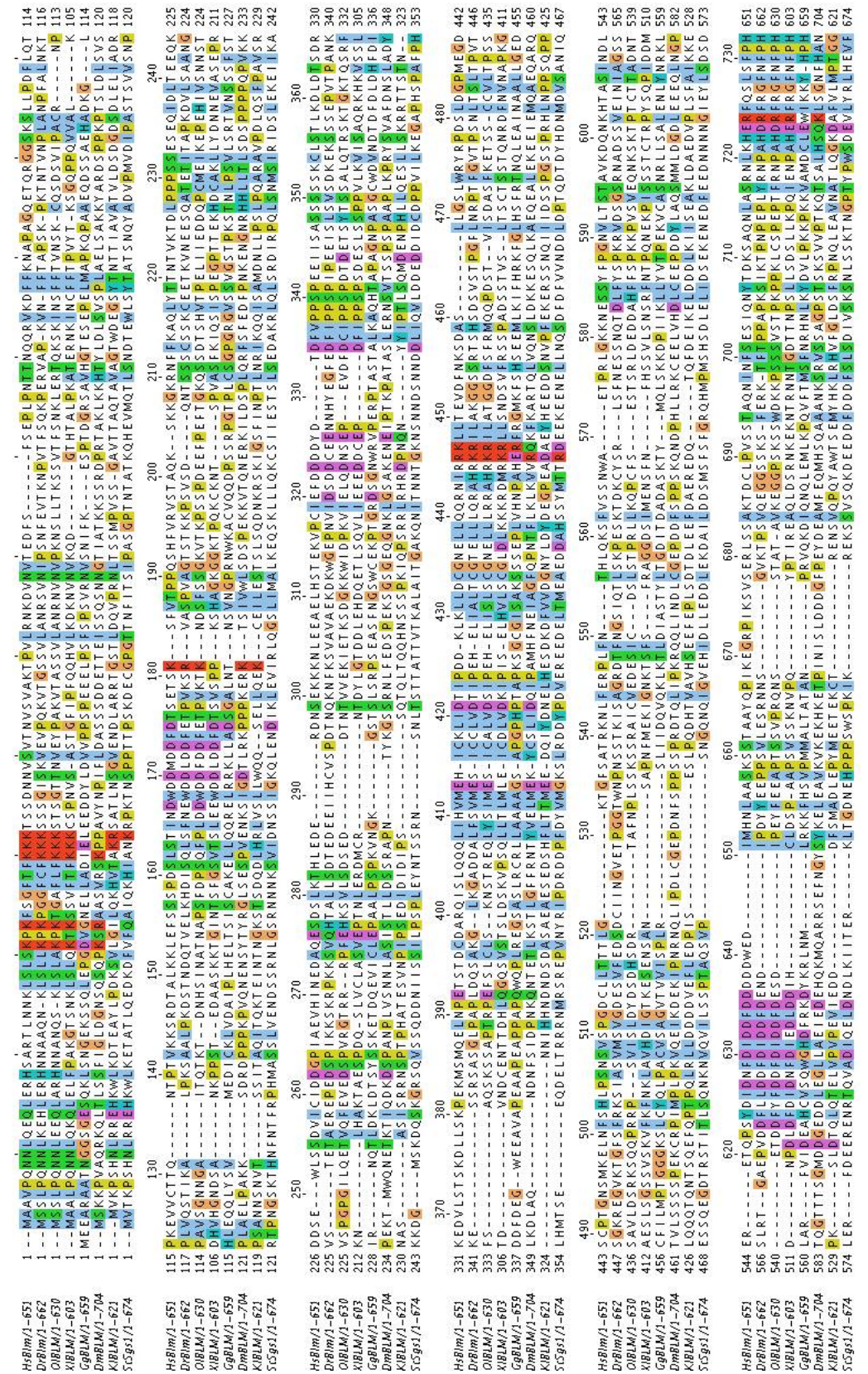

In the N-terminus, two acidic regions (AR1 and AR2) have been identified, most recently defined as spanning amino acids aa 321-474 and aa 502-648 respectively (Bernstein et al 2009). The N-terminus may be involved in mediating protein-protein interactions (Miyajima et al. 2000, Bernstein et al. 2009). It is also found to be in complex with Top3 and Rmi1 and there is evidence of physical interactions of the N-terminal half of Sgs1 with Top2 and Rad16, as illustrated in Figure 4 (reviewed in ref Bernstein et al. 2010).

Miyajima and colleagues report in their 2000 paper, the generation of several plasmids with deletions within *SGS1*, one of which they described as deleting the highly acidic region of amino acids 401-595 (i.e. slightly different from the most recent definitions). They transformed this plasmid into a *S.cerevisiae* yeast strain where the coding region for Sgs1 had been deleted (*sgs1*Δ) and tested it for: -a) MMS and HU sensitivity, b) recombination frequency between heteroalleles in the mitotic cell cycle, and c) sporulation defects and return-to-growth assay. They found that the yeast strain containing Sgs1 with the AR region deleted (*sgs1*-ARΔ) essentially behaved like wt *SGS1* in two assays: 1) the MMS and HU sensitivity assays 2) Mitotic recombination assay as tested through interchromosomal recombination between hetreoalleles, *his1-1/his1-7* in a diploid, detected via restoration of histidine prototrophy. In this assay, s*gs1*Δ had high levels of recombination as compared to wt Sgs1 and therefore *sgs1*-ARΔ suppressed the hyper recombination phenotype of s*gs1*Δ. However, in contrast, *sgs1*-ARΔ did not behave like wt in the meiotic functions tested. The authors showed that *sgs1*-ARΔ had reduced sporulation and reduced meiotic recombination (as tested by return-to-growth assay) in comparison to wt Sgs1. This reduction was not as severe as in the *S.cerevisiae* yeast strain where the coding region for Sgs1 had been completely deleted. Their results indicated that the 126-595

amino acid region is required for the complementation of poor sporulation and reduced meiotic recombination. (Miyajima et al. 2000)

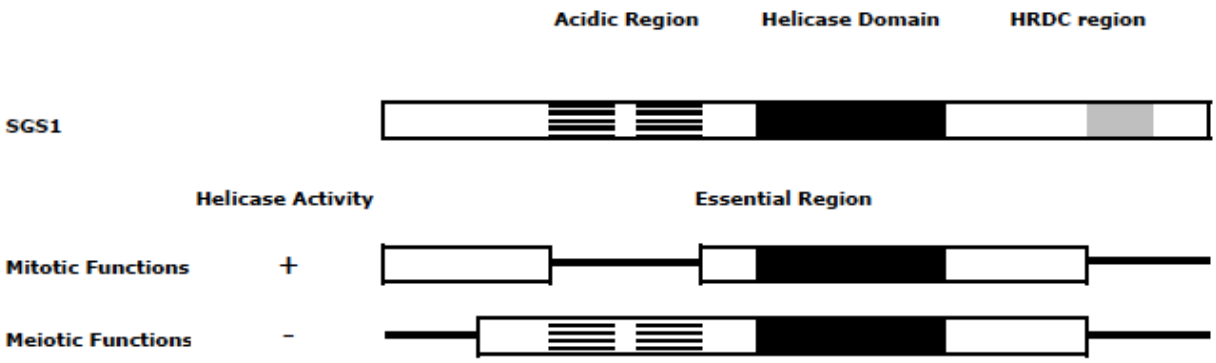

Figure 8. Schematic diagrams of domains of Sgs1 required for mitotic and meiotic functions. *The symbols, + and -, indicate to require and not to require helicase activity for the functions respectively. (Miyajima et al. 2000)*

Ui and colleagues in their 2001 paper tested many different missense mutations in Sgs1 and various deletion constructs of Sgs1 for MMS sensitivity and hyper-recombination. Amongst the results, which are summarized in Figure 9, they largely reconfirmed that the AR regions are not essential for suppression of MMS sensitivity or the suppression of hyper-recombination, as tested through interchromosomal recombination between hetreoalleles, *his1-1/his1-7* in a diploid. (Ui et al. 2001)

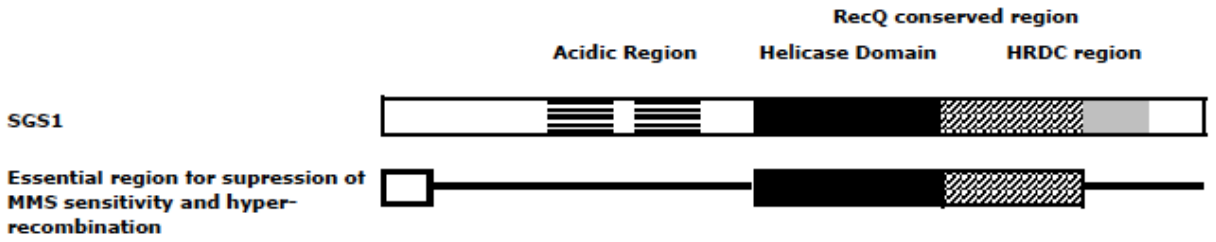

Figure 9. A summary of results from Ui et al 2001 paper obtained using deletion mutants.

Bernstein and colleagues in their 2009 paper also tested *sgs1* mutants in various assays, however in contrast to some methods above using plasmid borne deletions, they constructed yeast strains with chromosomal deletions in *sgs1* and various other genes. One assay they used is the prototypical phenotype of the *SGS1* loss-of-function alleles in the suppression of *top3*Δ slow growth (Gangloff et al. 1994). Top3 is essential for normal Sgs1 function. In a *top3*Δ mutant background, removal of the Sgs1 N terminus has an effect opposite to that of *sgs1*Δ*:* instead of suppressing *top3*Δ defects, it exacerbates them (Mullen et al, 2000). This detrimental effect is helicase dependent, as concomitant mutation of the catalytic lysine 706 in the *sgs1*-Δ*N* protein abolishes its toxicity in the *top3*Δ mutant (Mullen et al, 2000). This result suggests that deletion of the N terminus creates a 'hyper-active' Sgs1 helicase, one that causes greater damage in the absence of Top3 than the wild-type Sgs1 protein. Those results support a model, first proposed by Gangloff et al (1994), stating that a functional Top3 is needed to resolve toxic DNA structures created by the Sgs1 helicase. Bernstein et al 2009 described the phenotype associated with deleting the AR2 (amino acids 502-648, i.e. *sgs1-AR2*Δ) and found that a separation-of-function phenotype results: disruption of either *sgs1-AR2*Δ or *sgs1-AR1–2*Δ (Δ321-648) suppresses *top3*Δ slow growth, similar to the null *sgs1*Δ phenotype. In contrast, *sgs1-AR1*Δ (Δ321-474) only modestly suppresses the slow growth of *top3*Δ . Furthermore, in an otherwise wild-type background, *sgs1- AR2*Δ is fully functional in its resistance to MMS DNA damage and therefore behaves like wild type. *sgs1-AR1*Δ is also resistant to MMS DNA damage. They went on to construct a *sgs1-D664*Δ allele that they believed mirrored the separation-of-function of the *sgs1-AR2*Δ mutant and performed further assays that I will not describe here. The results of these assays solidified their view that Sgs1's function in the repair of DNA replication intermediates is separable from its role in homologous recombinational repair. (Bernstein et al. 2009)

Lastly, Mirzaei and colleagues suggests that the disordered N-terminus of Sgs1 is a site of protein binding and posttranslational modifications that confers species specificity to *BLM* and *SGS1*. This is their conclusion as a result of some very interesting experiments involving a *SGS1/BLM* chimera. Firstly they reconfirm some results of earlier researchers, such as the last 240 amino acids are dispensable to for resistance to MMS and HU. Even though Sgs1 is the homolog of *BLM*, the expression of a single copy of *BLM* did not complement *sgs1*Δ defects. *BLM* over- expression, however, significantly increased the rate of accumulating gross-chromosomal rearrangements in a dosage-dependent manner and greatly exacerbated sensitivity to DNA-damaging agents such as HU. Of interest to this paper, in order to determine if full-length Sgs1 was required for this suppression of *BLM* overexpression, the authors crossed the haploid strain over expressing *BLM* with haploids expressing various Sgs1 truncations. They found that a single copy of the *sgs1-*Δ*C200* allele was as sufficient as wild-type Sgs1 in suppressing HU sensitivity and slow growth of the *BLM* over-expressing strain, and as few as 547 N-terminal amino acids remaining in the *sgs1-*Δ*C900* allele were sufficient for significant suppression of HU sensitivity and slow growth caused by *BLM* overexpression. These findings suggest that none of the known enzymatic activities or functional and conserved domains are required for suppressing the HU sensitivity of the *BLM* over-expressing diploids but that 547 N-terminal amino acids are sufficient for suppressing the detrimental effects of *BLM* over-expression. This led the authors to consider constructing a Sgs1/*BLM* chimera and they used the IUPred algorithm (as described below) to help them design one. They constructed a yeast–human chimera in which the 647 N-terminal residues of *BLM* were replaced by the 647 N-terminal residues of Sgs1 (*sgs1*Δ *C800- blm*Δ *N647*). Surprisingly the chimera was nearly as effective as wild-type *SGS1* in conferring resistance to HU, and this chimera also showed partial suppression

of chromosomal rearrangement in *BLM* over-expressing cells. As a result of their experiments, they believe that *BLM* may possess helicase activity in yeast, leading to increased unwinding upon over expression, but it fails to elicit proper downstream responses, such as through a lack of specie specific proper N-terminal protein-protein interaction.

The N-terminus of both *BLM* and Sgs1 have been found to be significantly more disordered than ordered. Mirzaei and colleagues used IUPred, an algorithm for the prediction of intrinsically disordered proteins, and found that the 650 N-terminal residues contain a similar distribution of ordered and intrinsically disordered segments (Fig. 10). In disorder prediction algorithms, such as IUPred, a score of greater than 0.5 predicts a disordered amino acid residue and a score of less than 0.5 predicts an ordered residue, with 30 consecutive disordered amino acids commonly being used as a lower limit for detecting disorder in whole proteome searches. The helicase domains of Sgs1 and of *BLM* coincide with the predicted ordered regions in both proteins, starting at around residue 648, and are surrounded by a long N-terminal and a short C-terminal segment, which contain mostly disordered residues. In fact, based on the IUPred output scores, 83% of the 648 N-terminal residues of Sgs1 (538/648) are disordored, with 70% of all 648 residues being located in segments of more than 30 consecutive disordered residues, whereas only 16% of the 800 C-terminal residues of Sgs1 are predicted to be disordered, with only a single disordered segment that is longer than 30 residues (residues 1396–1447). Based on the IUPred prediction, *BLM* can also be divided into a disordered N- terminus and an ordered C-terminus (Fig. 10). For *BLM*, 52% of 648 N-terminal residues are predicted to be disordered, but only 15% of these residues are found in stretches of more than 30 disordered residues. While investigating *BLM's* ability to complement *sgs1*Δ defects, Mirzaei and colleagues used the above computational protein disorder prediction tool to design and yeast-human chimera (*sgs1*ΔC800-

blm ΔN647) to suppress *sgs1*Δ defects. They found that their results suggested a functional relationship between *BLM* and Sgs1 as the chimera suppressed the severely detrimental effects of *BLM* overexpression in yeast, as detailed previously (Mirzaei et al. 2011).

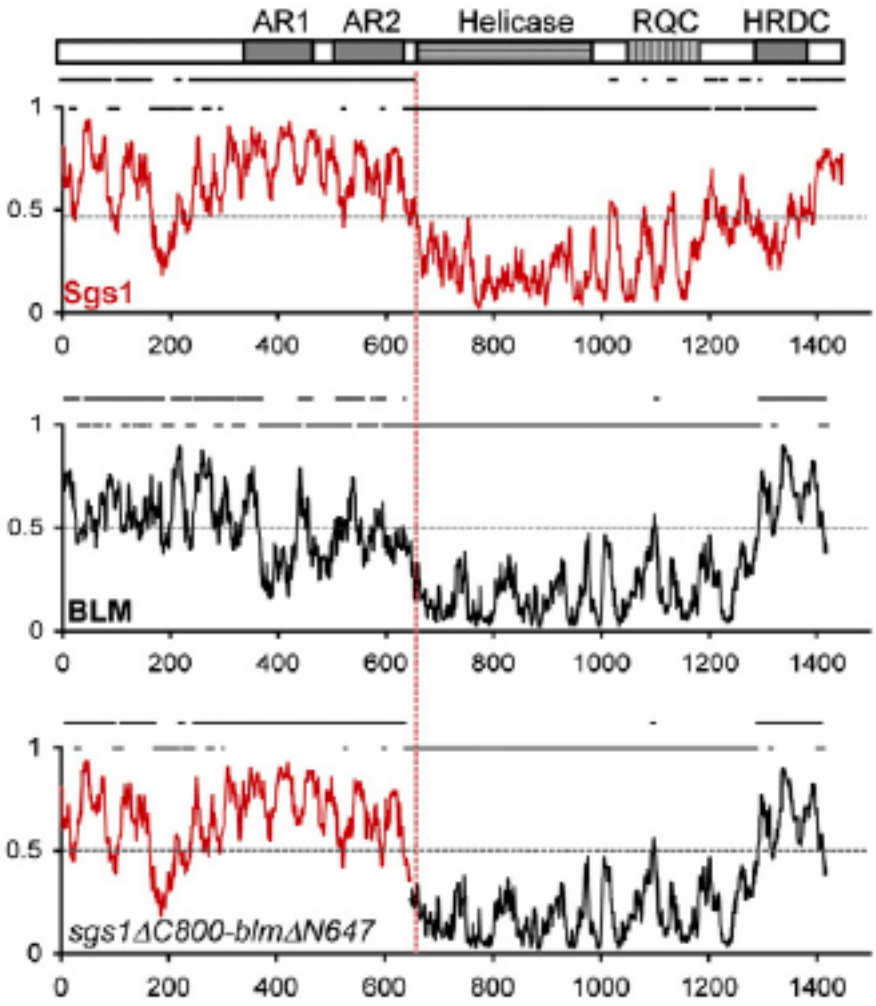

Figure 10. IUPred algorithm* for SGS1, BLM *and SGS1/BLM chimera.
Construction of a functional chimerical protein composed of the N-terminus of Sgs1 and the C-terminus of BLM. *Protein disorder prediction of Sgs1 (red) and* BLM *(black), using the IUPred algorithm. Values above 0.5 indicate a disordered residue, whereas values below 0.5 indicate ordered residues; amino acid residue numbers (1–1447) are indicated on the abscissa. Black lines above the graph show a simplified order and disorder distribution along the length of the protein with values above 0.5 being assigned a "1" and values below 0.5 being assigned a "0". The vertical red line indicates the site in Sgs1,* BLM*, and the chimera where the disordered N-terminal segment transitions into the ordered helicase domain at residues 647–648. This site was chosen as the fusion site for the chimera. The approximate location of Sgs1 domains is indicated above . Disorder prediction for the Sgs1–BLM chimera in which the 647 N-terminal residues of* BLM *(black) were replaced with the 647 N-terminal residues of Sgs1 (red) (Mirzaei et al. 2011).*

SUMMARY

Apart from the DNA helicase domain, *BLM/SGS1* orthologs contain a poorly characterized N-terminal domain of about 650 amino acids (aa) (Fig. 7a). There is lack of sequence conservation between orthologs of the N-terminus and as a result this has hindered its functional analysis. (Fig. 7b) In yeast, this domain (Sgs1 1-652) is known to be physiologically important (Mullen et al. 2000) although it's only known roles are to bind Top3 and Rmi1 through its N-terminal 100 aa, and *in vitro* single-strand DNA (ssDNA) binding, ssDNA annealing and strand exchange (SE) activities, through its SE domain (Sgs1 103-323).

The domain of Sgs1 aa323- 622 remains largely uncharacterized. There are many structure/function analyses that have been performed in this area. Generally this domain has been shown to be dispensable for mitotic functions, suppression of MMS sensitivity and hyper-recombination, and essential for meiotic functions (Miyamjima et al. 2000, Ui et al. 2001). Furthermore, Bernstein and colleagues, believe that the AR2 (aa 502-648) region is physiologically important as they present assay results that illustrate a separation of function in repair of DNA replication intermediaries and its role in homologous recombinational repair (Bernstein et al. 2009).

My goal was to interrogate this region by doing systematic deletions, test these *sgs1* mutants for complementation of synthetic lethality, and define an essential domain in order to help elucidate a function or structure for this uncharacterized area. The allele with the smallest deletion that did not complement *sgs1slx4* synthetic lethality was found to be *sgs1-Δ386-621,* and in *the sgs1slx5* background, *sgs1-Δ500-621.* The results of this assay, was then compared to the current published data, to take note of any differences. This comparison will help determine

the next assays to complete, to further characterize this region of Sgs1 between the helicase and SE domain.

Results and Discussion

On a Clustal W alignment of *BLM* orthologs (Fig. 10) there is marked sequence conservation in the C terminus of *BLM* orthologs including Sgs1 that includes the Helicase domain, RecQ domain and HRDC domain. In the N terminus there is little conservation except for a domain named BDHCT, which spans *BLM* aa 371-411. A search in the pfam database was performed for *BLM* BDHCT family members, and 5 orthologs for BDHCT (Fig 11), all in mammalian genomes were identified. However a BDHCT domain in Sgs1 or other single celled eukaryotes was not identified. A function has not been ascribed to the BDHCT region however as it is conserved, using the Clustal W alignment of BLM, a putative essential region was mapped to Sgs1 and a plasmid was constructed for *sgs1*-Δ*386-428*. One of the most sensitive assays for *SGS1* function is its ability to complement *sgs1*Δ *slx*Δ synthetic lethality (Mullen et al. 2001). This *sgs1*-Δ*386-428* mutant, plasmid No.1618 (p1618), was tested in two strains, *sgs1*Δ *slx4*Δ and *sgs1*Δ *slx5*Δ*,* that are kept alive by plasmid pJM500 (*SGS1/URA3/CEN*). Both strains were transformed with plasmid-borne *sgs1*-Δ*386-428*, and the transformants were then streaked onto media that selects against pJM500, 5-FOA. Transformants with plasmid borne sgs1-Δ386-428 grew identical to wt *SGS1* and therefore complemented both strains. As a result the putative BDHCT domain of Sgs1 aa386-428 is considered nonessential to *SGS1* function. (Fig. 12)

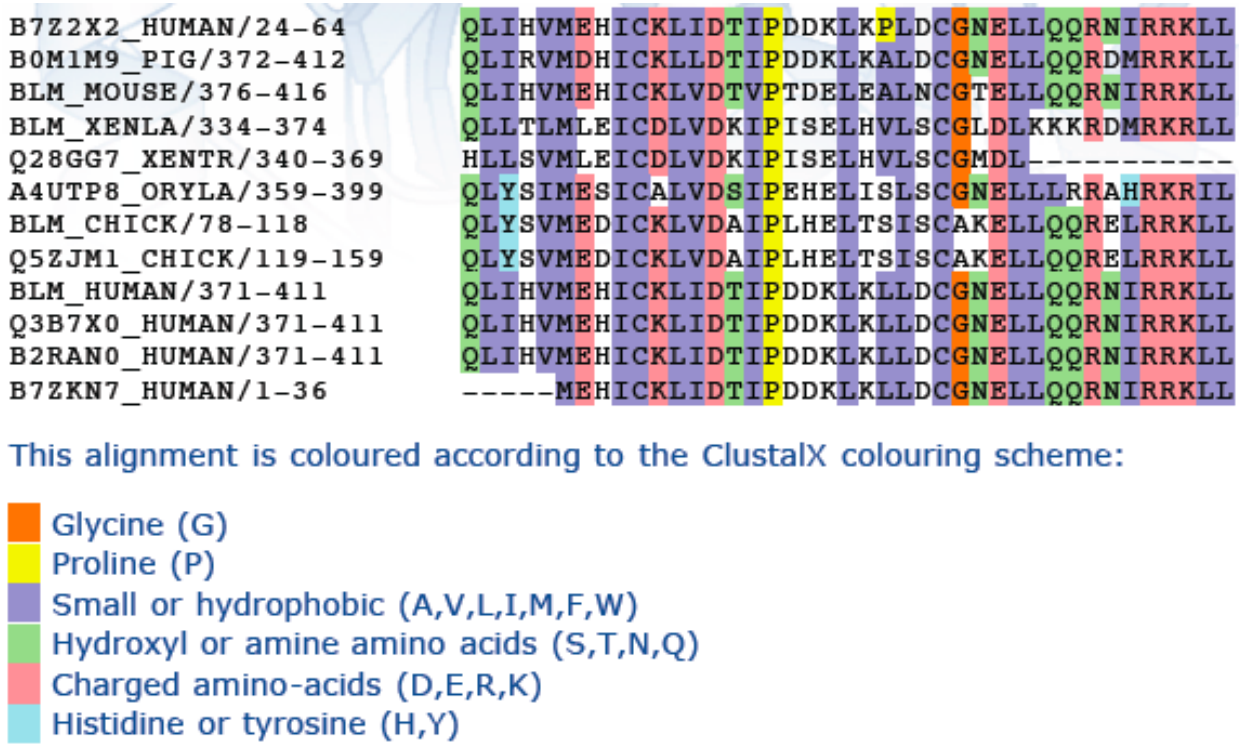

Figure 11. Pfam search results for* BLM *BDHCT (PF08072) family members *(http://pfam.sanger.ac.uk/family/bdhct#tabview=tab0). Results include proteins from Human, Pig, Mouse, XENLA (African clawed frog), Orylag (Rabbit) and Chicken*

As previously mentioned, other assays have been completed to elucidate the structure and function of Sgs1 in the region of aa 323-652, but to my knowledge this area has not been tested for its ability to complement synthetic lethality. In an attempt to characterize this region and as the putative BDHCT region (aa 386-428) is nonessential, a plasmid was constructed which deleted from the putative BDHCT region to the Helicase region (Δ429 -652). This plasmid (p1620) borne *sgs1*-Δ*429 -652* mutant was transformed into two yeast strains (*sgs1*Δ *slx4*Δ and *sgs1*Δ *slx5*Δ) and then streaked onto media that contained 5-FOA which selects against pJM500 (*SGS1/URA3/CEN*). This deletion did not complement synthetic lethality in either strain as it did not grow on media that contained 5-FOA. Therefore this domain (aa 429 -652) is considered essential (Fig. 12).

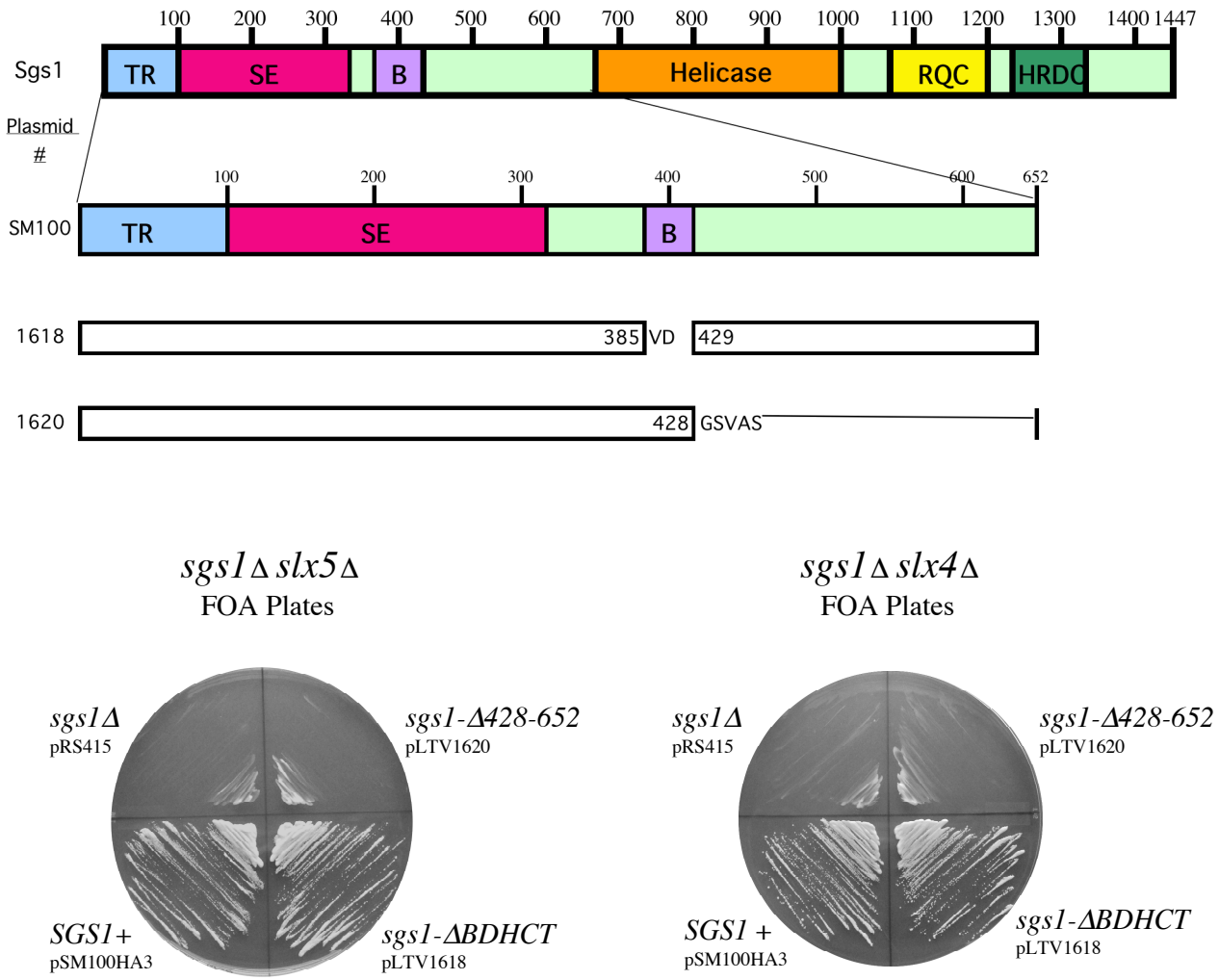

Figure 12. Synthetic lethal assay for plasmids p1618 and p1620. *(a) Schematic alignment of Sgs1 and internal deletions. Sgs1 functional domains:- TR –Top3/Rmi1 binding domain. SE – Strand Exchange. B- putative BDHCT. RQC-RecQ C-terminal. HRDC- RNAseD C-terminal. Plasmid's and aa deletions schematically represented and aa and plasmid #'s noted (b) Strains NJY2083* (sgs1–11::loxP slx4–11::loxP *plus pJM500* (SGS1/ URA3/ADE3/CEN*)) and NJY2924* (sgs1–20::HGR slx5-10::TRP1 *plus pJM500) were transformed with various* SGS1 *alleles in pRS415 as indicated in the key. Transformants were streaked onto plates containing 5-FOA and the plates were photographed after 2 (*sgs1Δ slx4Δ*) or 3 (*sgs1Δ slx5Δ*) days growth at 30°C*

These two alleles were then tested for their ability to complement the MMS sensitivity of *sgs1*Δ and both alleles, *sgs1*-ΔBDHCT and *sgs1*-Δ *428-652,* conferred wt-level of resistance (Fig. 13). This result is consistent with Ui and colleagues results showing that *SGS1* alleles with deletions within the Sgs1 N-terminus are resistant to MMS DNA damage (Ui et al. 2001).

Figure 13. MMS sensitivity assay for p1618 and p1620 *Strain NJY1460 (*sgs1Δ) *was transformed with the indicated* SGS1 *deletions and resuspended at OD=3, serially diluted in three- fold increments and approximately 5ul were spotted onto -LEU plates with or without 0.03% MMS. Plates were photographed after 2 (-LEU) or 3 days (MMS) growth at* 30^0C

Figure 13.

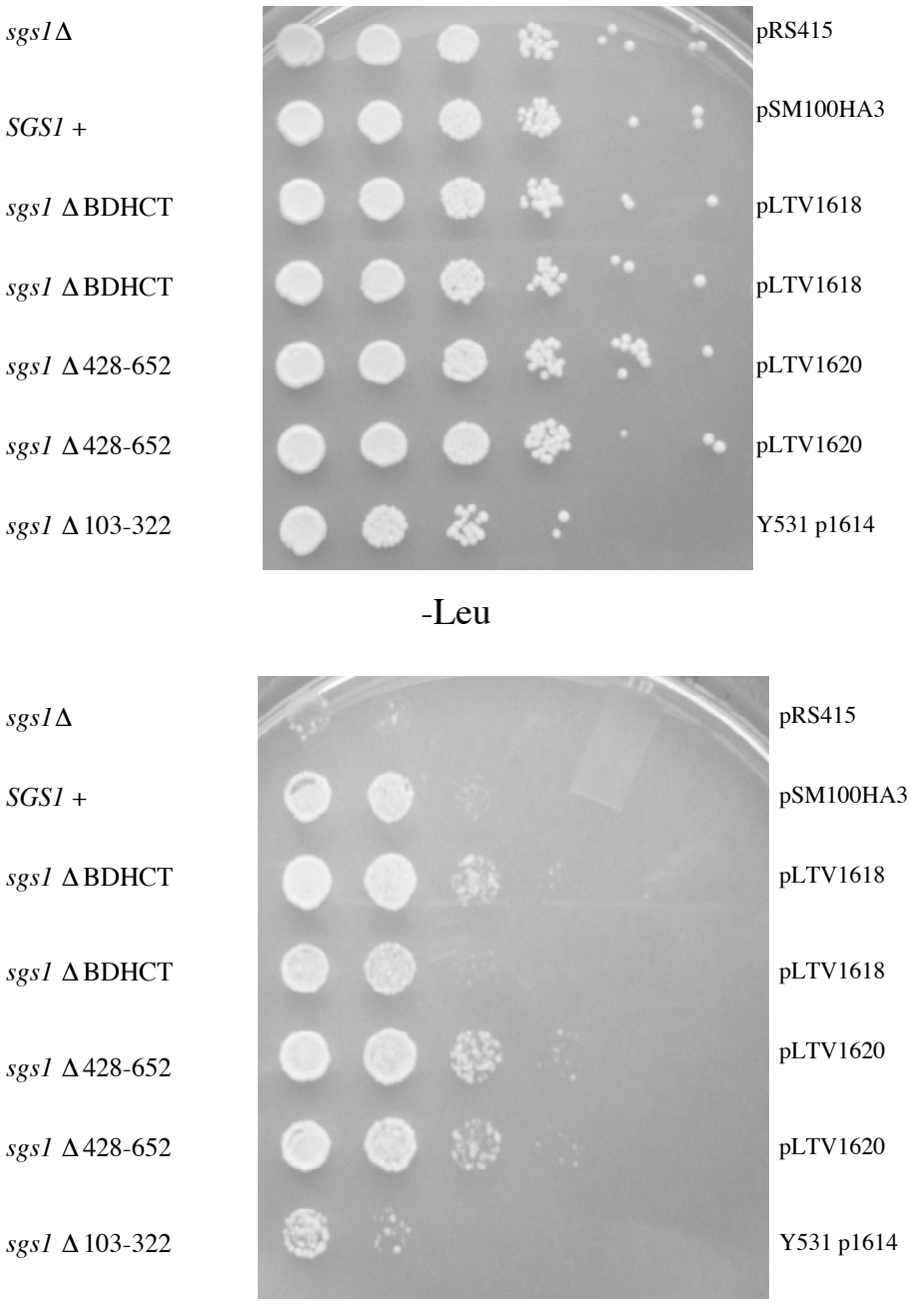
sgs1Δ
SGS1 +
sgs1 ΔBDHCT
sgs1 ΔBDHCT
sgs1 Δ428-652
sgs1 Δ428-652
sgs1 Δ103-322
pRS415
pSM100HA3
pLTV1618
pLTV1618
pLTV1620
pLTV1620
Y531 p1614
-Leu
sgs1Δ
SGS1 +
sgs1 ΔBDHCT
sgs1 ΔBDHCT
sgs1 Δ428-652
sgs1 Δ428-652
sgs1 Δ103-322
pRS415
pSM100HA3
pLTV1618
pLTV1618
pLTV1620
pLTV1620
Y531 p1614
MMS (0.03%)

The deletion of aa 428-652 (p1620) is large and an argument could be made that it might not be essential, as it could just be destabilizing the protein or somehow be interfering with the helicase region, as this deletion abuts this area. However, as it is not MMS sensitive then the helicase is probably functional, but it still would be desirable to try to pin point a smaller deletion that would not complement synthetic lethality. Therefore a systematic series of 20 different deletions were made and plasmid borne *sgs1* mutants were transformed into the two yeast strains, *sgs1*Δ *slx4*Δ and *sgs1*Δ *slx5*Δ, that are kept alive by plasmid pJM500 (*SGS1/URA3/CEN*) and tested for synthetic lethality as described in Mullen et al. 2001. All the internal deletions that were constructed are listed in the Supplemental figures (Sup. Fig. 1. and Sup. Fig. 2.) and their results in the synthetic lethality assay noted.

The minimum essential region as detailed in deletion mapping from the left side is aa 386-621 (p1626) (Fig. 14). This mutant confers resistance to MMS sensitivity, however at levels less than wt (Fig.15a.) Interestingly a slightly larger deletion, Δ386-652 (p1627), that deletes aa up to the helicase region seems to confer better resistance to MMS sensitivity than *sgs1*-Δ*386-621*. However these two deletions, *sgs1*-Δ*386-621* and *sgs1*-Δ*386-652*, confer similar results in the *top3* slow growth assay (Fig 15b.).

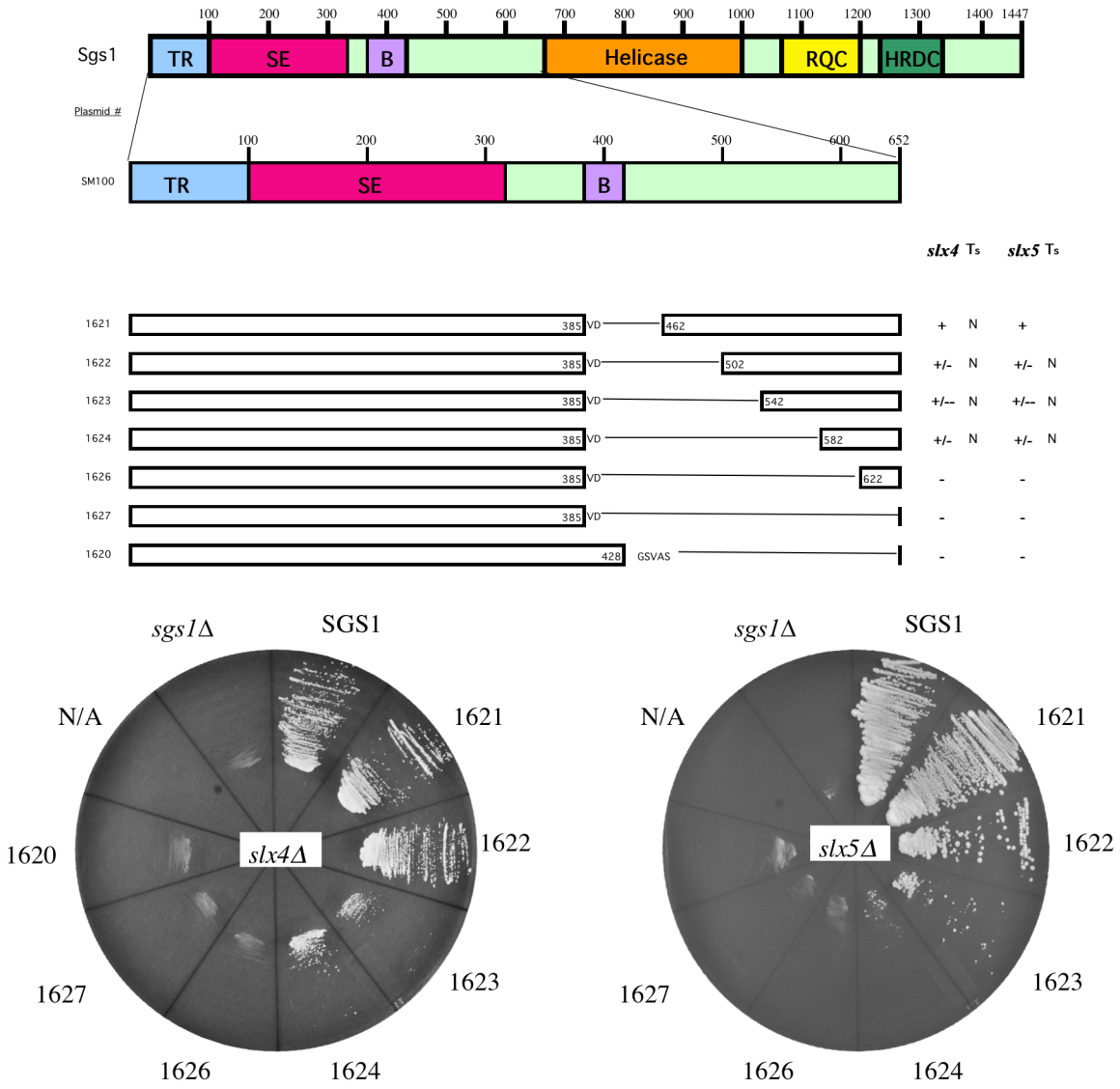

Figure 14. Synthetic lethal assay for p1621, p1622, p1623, p1624, p1626, p1627, p1620 *(a) Schematic alignment of Sgs1 and internal deletions. Sgs1 functional domains:- TR –Top3/Rmi1 binding domain. SE –Strand Exchange. B- putative BDHCT. RQC-RecQ C-terminal. HRDC-RNAseD C-terminal. Plasmid's and aa deletions schematically represented and aa and plasmid #'s noted (b) Strains NJY2083 (*sgs1–11::loxP slx4–11::loxP *plus pJM500 (*SGS1/ URA3/ADE3/CEN*)) and NJY2462 (*sgs1–11::HGR slx5Δ::NAT *plus pJM500) were transformed with various* SGS1 *alleles in pRS415 as indicated in the key. Transformants were streaked onto plates containing 5-FOA and the plates were photographed after 2 (*sgs1Δ slx4Δ*) or 3 (*sgs1Δ slx5Δ*) days growth at 30°C*

Figure 15. MMS and* Top3 *slow growth assay for p1626 and p1627. *(a) Strain NJY1460 (*sgs1Δ*) was transformed with the indicated* SGS1 *deletions and resuspended at OD=3, serially diluted in three- fold increments and approximately 5ml were spotted onto YPD plates with or without 0.03% MMS. Plates were photographed after 1 (YPD) or 3 days (MMS) growth at 30^0C. (b) Strain NJY728 (sgs1Δ top3Δ plus pJM555* (TOP3/URA3/ADE3/CEN)*) was transformed with the indicated* SGS1 *alleles in pRS415 (*LEU2/CEN*). Transformants were streak purified on SD-leu plates, resuspended to OD600 = 3.0 and serially diluted in three-fold increments. Approximately 5ml were spotted onto SD plates lacking leucine but with or without 5-FOA. Plates were photographed after 1 (-Leu) or 3 (5-FOA/ Leu) days growth at 30^oC.*

Figure 15a. MMS assay

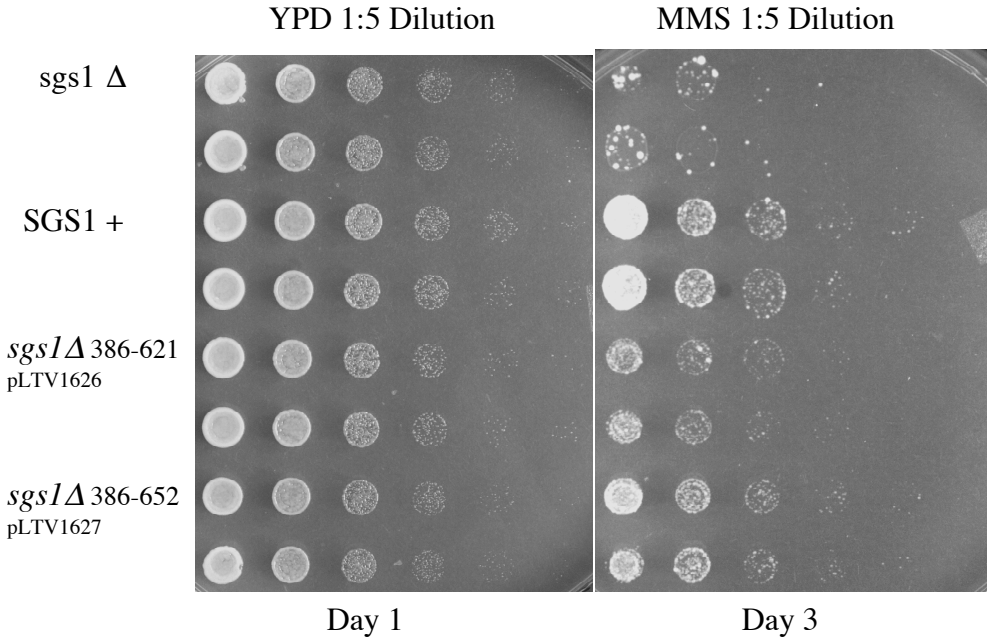

Figure 15b. Top3 slow growth assay

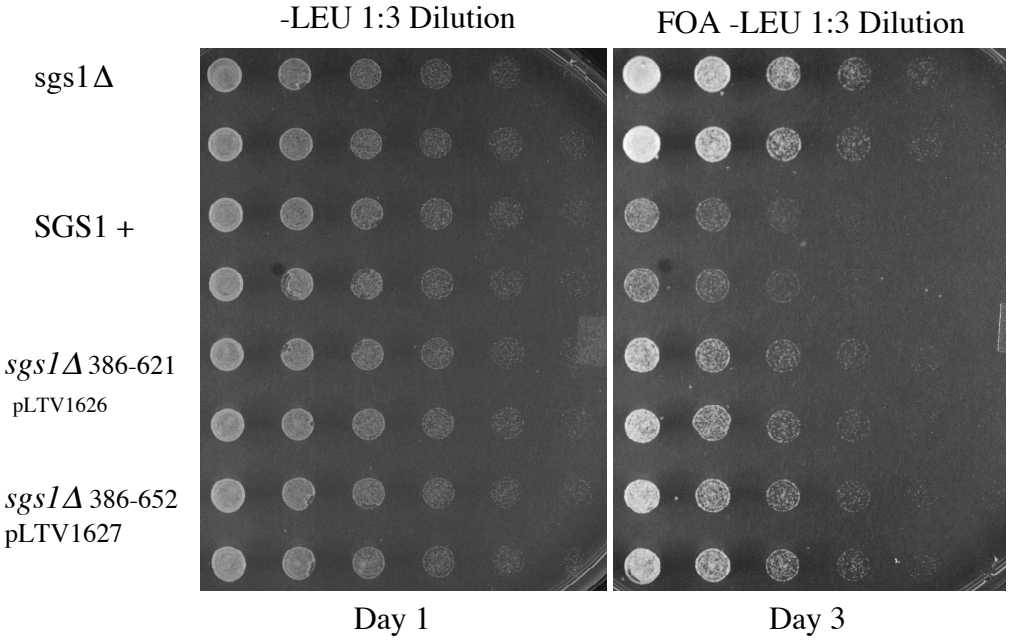

The prototypical phenotype of *SGS1* loss-of-function alleles is the suppression of *top3*Δ slow growth (Gangloff, McDonald et al. 1994). However some separation of function alleles, such as *sgs1-D664*Δ, confer this phenotype as well (Bernstein et al. 2009). To test the effect of the alleles, *sgs1*-Δ*386-621* and *sgs1*-Δ*386-652,* in the *top3*Δ background, we introduced the plasmid-borne *SGS1* alleles into an *sgs1*Δ *top3*Δ double mutant that contained plasmid pJM555 (*TOP3/URA3/CEN*). These strains were then serially diluted and spotted onto medium containing 5-FOA, which selects against pJM555. As expected, the *sgs1*Δ allele allowed good growth on this medium while *SGS1* promoted slow growth (Fig. 15b). The alleles of *sgs1*-Δ*386-621* and *sgs1*-Δ*386-652* behaved like *sgs1*Δ*,* as indicated by the good growth of this strain on 5-FOA. Based on this data, *sgs1*-Δ*386-621* and *sgs1*-Δ386-652 resembles *sgs1-D664*Δ in that these alleles suppress *top3*Δ slow-growth but remain MMS resistant.

A further series of deletions mapping from the right side were constructed (Sup. Fig. 1. and Sup. Fig. 2.) and tested in the synthetic lethality assay and the allele with smallest deletion that did not complement the synthetic lethality remained *sgs1*Δ386-621. Alleles with smaller deletions, as constructed in plasmids 1644, 1643,1642,1641,1648,1649,1650 (Sup. Fig. 1. and Sup. Fig. 2.), did complement synthetic lethality but grew weakly in the *sgs1*Δ *slx4*Δ yeast strain. However these alleles did not complement synthetic lethality in the *sgs1*Δ *slx5*Δ yeast strain. The growth rate of *sgs1*Δ *slx5*Δ is slower than *sgs1*Δ *slx4*Δ (Mullen et al. 2001) and therefore the difference in results between *sgs1*Δ *slx4*Δ and *sgs1*Δ *slx5*Δ strains was not considered significant.

When the results of the deletions I have constructed are compared to the effects of mutations in the AR2 region identified as important by Bernstein and colleagues, there are

differences between their results and ours. In Fig 16 we show that our allele (*sgs1*-Δ*500-622*) that most closely matches the AR2 chromosomal deletion (*sgs1*-Δ*502-648)* in Bernstein's paper, does grow weakly in the *sgs1*Δ *slx4* background. Therefore this region in the synthetic lethality assay is considered nonessential, as opposed to Bernstein and colleagues conclusion that it is important. We note the approximate location of the AR2 region in Figure 16. Furthermore, the fact that this allele (*sgs1*-Δ*500-622)* and alleles with larger deletions (S. Fig.2) do not survive in an *sgs1*Δ *slx5* background, but do survive in the *sgs1*Δ *slx4*Δ background merits further investigation. The Slx1-Slx4 complex acts as a Holiday Junction resolvase (Svendsen et al. 2010) and Slx5-Slx8 complex is a Sumo-targeted Ubiquitin ligase (Mullen et al. 2010). These protein's disparate functions and our different results in the two backgrounds may help elucidate a function to this region between the SE and helicase domains. To begin with, the alleles with plasmids 1644, 1643,1642,1641,1648,1649,1650 should all be tested for MMS sensitivity and suppression of Top3 slow growth.

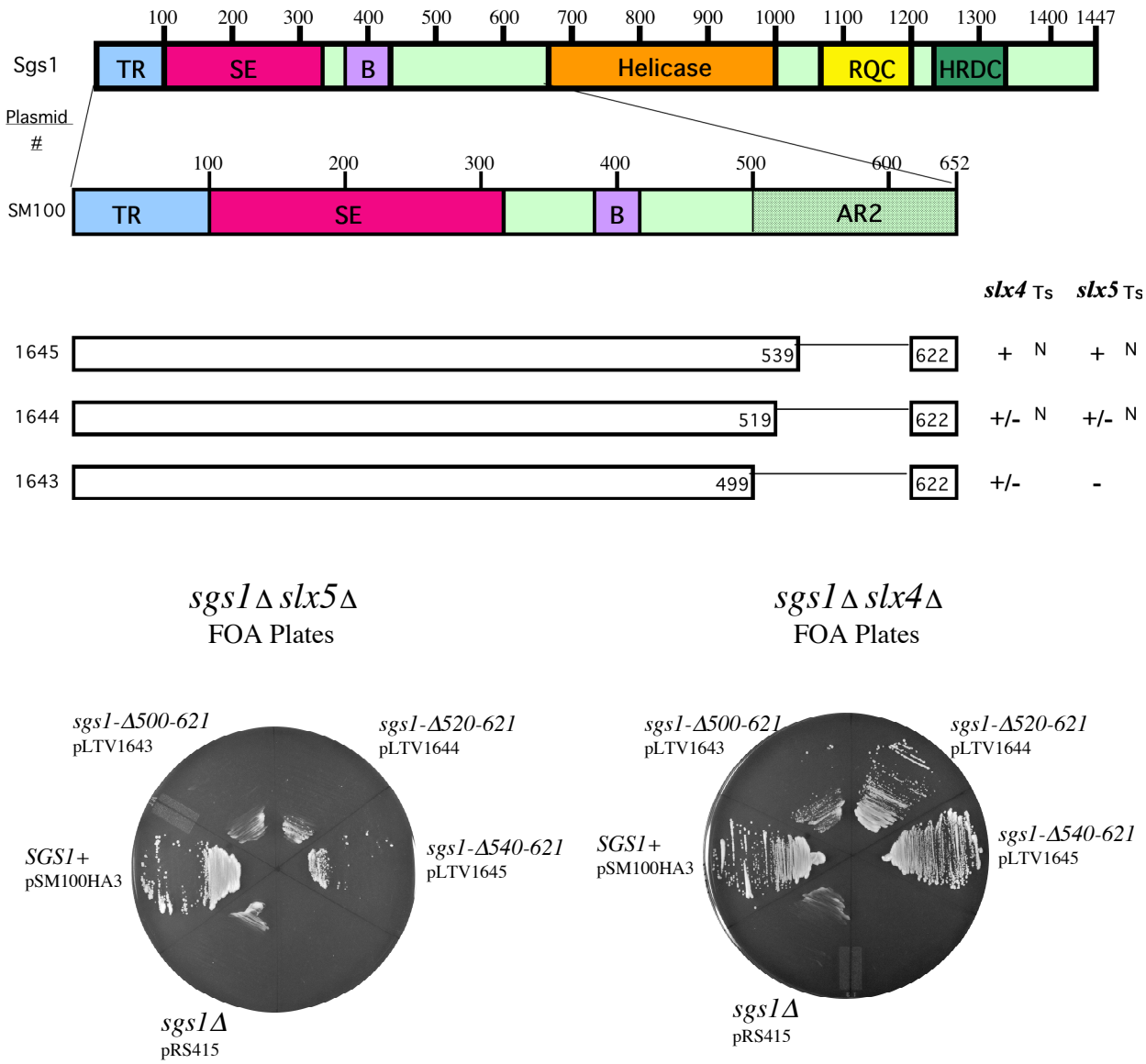

Figure 16. Synthetic lethal assay for p1645, p1644, p1643. *(a) Schematic alignment of Sgs1 and internal deletions. Sgs1 functional domains:- TR –Top3/Rmi1 binding domain. SE –Strand Exchange. B- putative BDHCT. RQC-RecQ C-terminal. HRDC- RNAseD C-terminal. Bernstein's and colleagues (2009) region AR2 (*sgs1-Δ502-648*) is also approximately noted. Plasmid's and aa deletions noted (b) Strains NJY2083* (sgs1–11::loxP slx4–11::loxP *plus pJM500 (*SGS1/ URA3/ADE3/CEN*)) and NJY2462 (*sgs1–11::HGR slx5Δ::NAT *plus pJM500) were transformed with various* SGS1 *alleles in pRS415 as indicated in the key. Transformants were streaked onto plates containing 5-FOA and the plates were photographed after 2 (*sgs1Δ slx4Δ*) or 3 (*sgs1Δ slx5Δ*) days growth at 30°C*

In an effort to further define a phenotype for some of these *sgs1* mutants, we tested whether the function of *sgs1-Δ429-651*, or *sgs1-Δ386-621* in the synthetic lethality assay, could be restored by replacing the deleted sequences with *BLM* or *WRN*. When the SE domain was replaced by *BLM* aa 95-300 function was restored and this chimera complemented synthetic lethality of both *sgs1Δ slx4Δ* and *sgs1Δ slx5Δ* (Chen et al. 2010). Chimera's were constructed such that *BLM* aa 412-628 replaced *SGS1* aa 429-651 and *WRN* aa 282-526 replaced *SGS1* aa 386-621. Neither chimera was able to restore function to the *sgs1* mutants. (Fig.17).

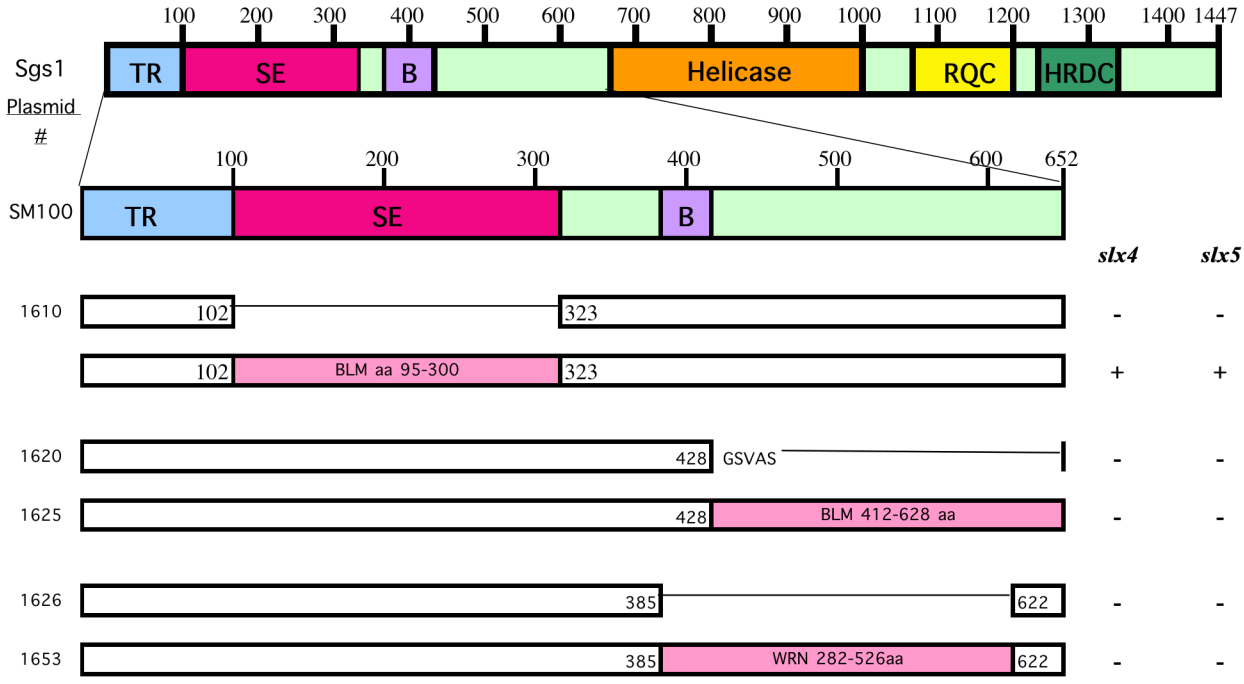

***Figure 17. Schematic for synthetic lethal assay for* BLM *and* WRN *chimera's with* SGS1.** *Schematic alignment of Sgs1 and internal deletions. Sgs1 functional domains:- TR –Top3/Rmi1 binding domain. SE –Strand Exchange. B- putative BDHCT. RQC-RecQ C-terminal. HRDC-RNAseD C-terminal. Plasmid's and aa deletions schematically represented and results in* sgs1Δ slx4Δ *or* sgs1Δ slx5Δ *yeast strains noted.*

Chen et al 2010 assayed proteins of the N-terminus of Sgs1 for various binding activities. They localized the minimal region required for ssDNA (174 deoxyoligonucleotide) binding activity to $Sgs1_{103-322}$ (subsequently labeled SE domain). To further investigate the N-terminus of Sgs1 in the area of interest for this thesis, we assayed various N-terminal proteins for its ability to bind various DNA substrates through performing electrophoretic mobility shift assays (EMSA). In Fig. 18 GST-fusion proteins of $Sgs1_{1-652}$ sub-domains were assayed for binding to P-32 labeled polydT 174. None of theses proteins, $Sgs1_{323-652}$, $Sgs1_{484-652}$ or $Sgs1_{103-250}$ bound the ssDNA. In Figure 19 we assayed $Sgs1_{323-652}$ (which includes our smallest essential region found of aa 386-621) for its ability to bind P-32 labeled D-Loop or HJ DNA substrates and found there was no binding. Therefore the N-Terminal essential domain of Sgs1 that I have been attempting to find a phenotype for, does not bind the DNA substrates described.

In Figure 20 we assayed the whole N-Terminus ($Sgs1_{1-652}$) for binding to the P-32 labeled D-Loop or HJ DNA substrates and confirmed that this GST-fusion protein does bind however at the expected higher protein concentrations than a GST-fusion protein that included the helicase region, $Sgs1_{400-1268}$. It was noted that $Sgs1_{1-652}$ bound the D-Loop and HJ DNA substrates at approximately the same concentration as $Sgs1_{103-322}$ (SE domain). This was unexpected as it was included in the assay as a negative control. Previous unpublished data (Chen and Brill) had suggested that the SE domain did not bind these DNA substrates. Therefore we titrated $Sgs1_{103-322}$ and $Sgs1_{1-652}$ and assayed for binding to P-32 HJ (Fig 21) and found that for $Sgs1_{103-322}$, higher protein concentrations were needed for HJ binding than for d(T)174. We also noted that compared to $Sgs1_{103-322}$, much lower protein concentrations of $Sgs1_{1-652}$ were needed for binding to the HJ.

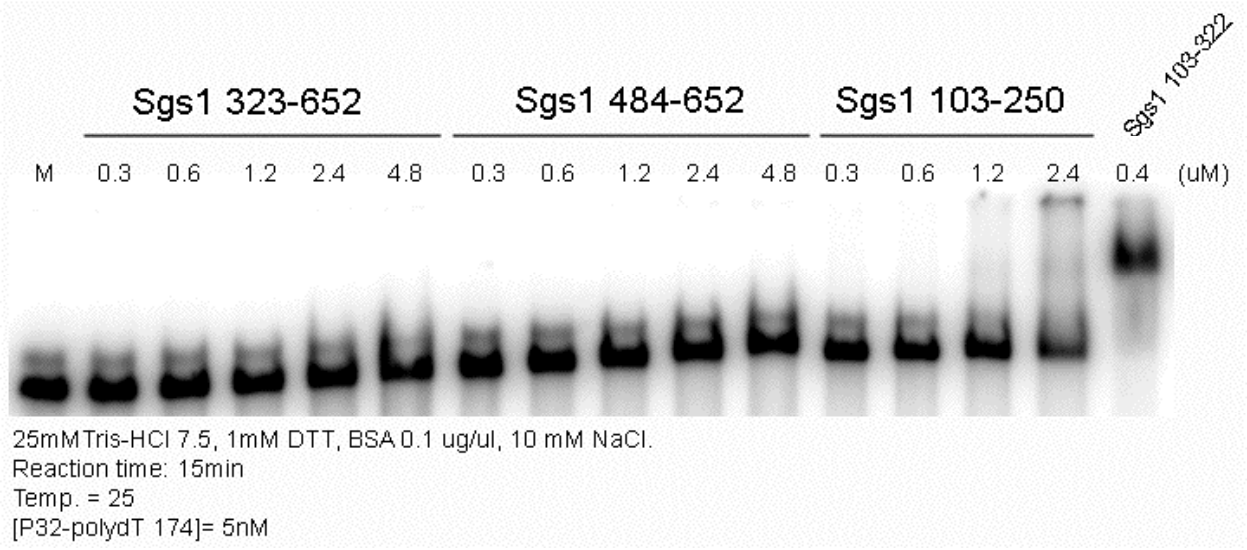

Figure 18. The lack of ssDNA binding activity of Sgs1$_{323-652}$, Sgs1$_{484-652}$ or Sgs1$_{103-250}$. *The above GST–Sgs1 fusion proteins were subjected to EMSA assay using ^{32}P-labelled poly(dT)174 as probe. GST–Sgs1$_{103-323}$ fusion protein (SE domain) included as a positive control.*

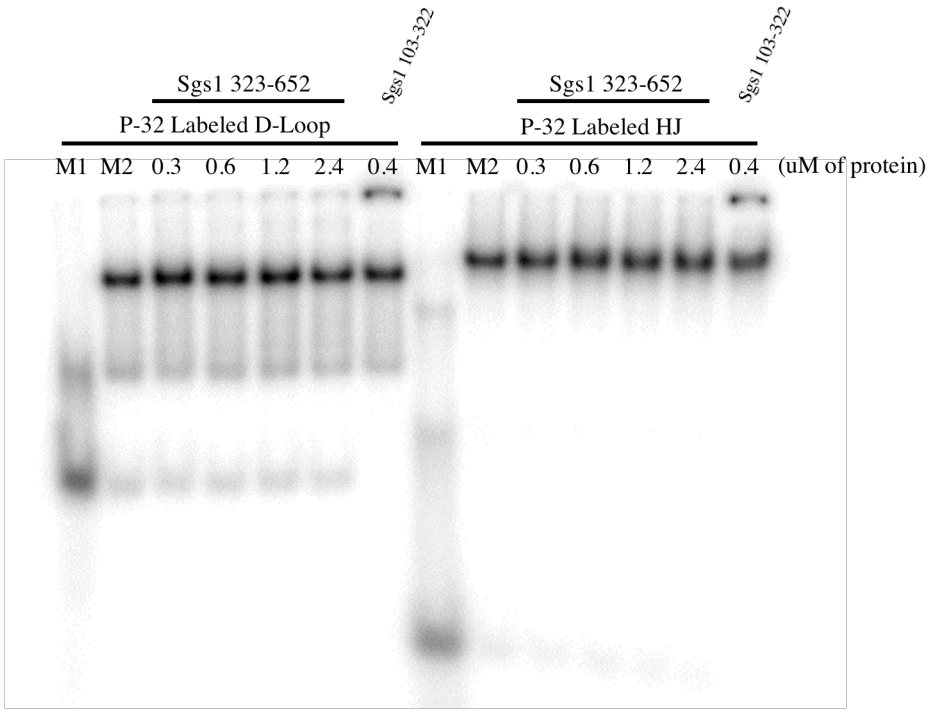

25mM Tris-HCl 7.5, 1mM DTT, BSA 0.1 ug/ul, 10 mM NaCl
Reaction Time: 15 min, Temp 25
[P-32 D-Loop 1nM] or [P-32 Holiday Junction 1nM]
M1 - Boiled D-Loop or HJ for 3 min - no protein
M2 - D-Loop or HJ alone - no protein

Figure 19. The lack of DNA substrate (D-Loop and HJ) binding activity of Sgs1 $_{323-652}$. *The above GST–Sgs1 fusion protein was subjected to EMSA assay using ^{32}P-labelled DNA oligo substrates of D-Loop or HJ as a probe. . GST–Sgs1$_{103-323}$ fusion protein (SE domain) included as a positive control.*

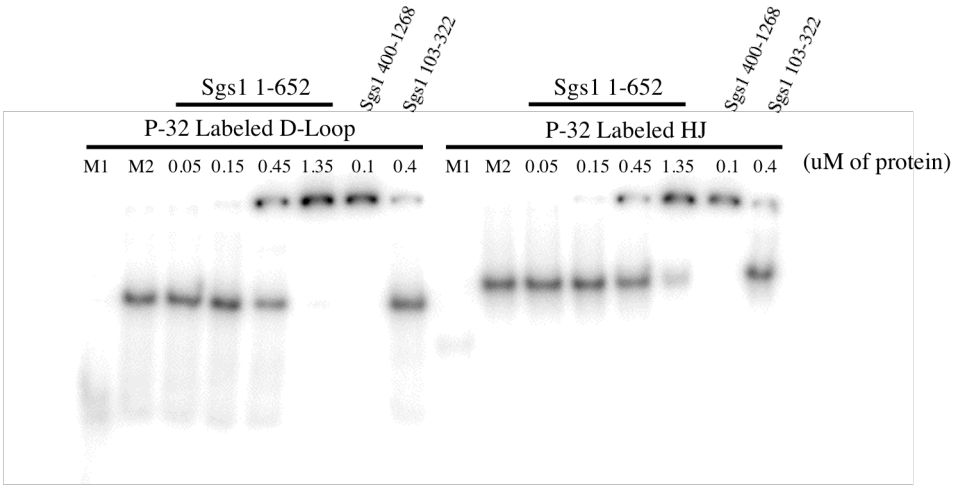

25mM Tris-HCl 7.5, 1mM DTT, BSA 0.1 ug/ul, 10 mM NaCl
Reaction Time: 15 min, Temp 25
[P-32 D-Loop 1nM] or [P-32 Holiday Junction 1nM]
M1 - Boiled D-Loop or HJ for 3 min - no protein
M2 - D-Loop or HJ alone - no protein

Figure 20. The DNA substrate (D-Loop and HJ) binding activity of N-terminal Sgs1$_{1-652}$. *The above GST–Sgs1 fusion protein was subjected to EMSA assay using ^{32}P-labelled DNA oligo substrates of D-Loop or HJ as a probe. GST–Sgs1$_{103-323}$ fusion protein (SE domain) included as a negative control in comparison to GST–Sgs1$_{400-1268}$ fusion protein included as a strongly positive control.*

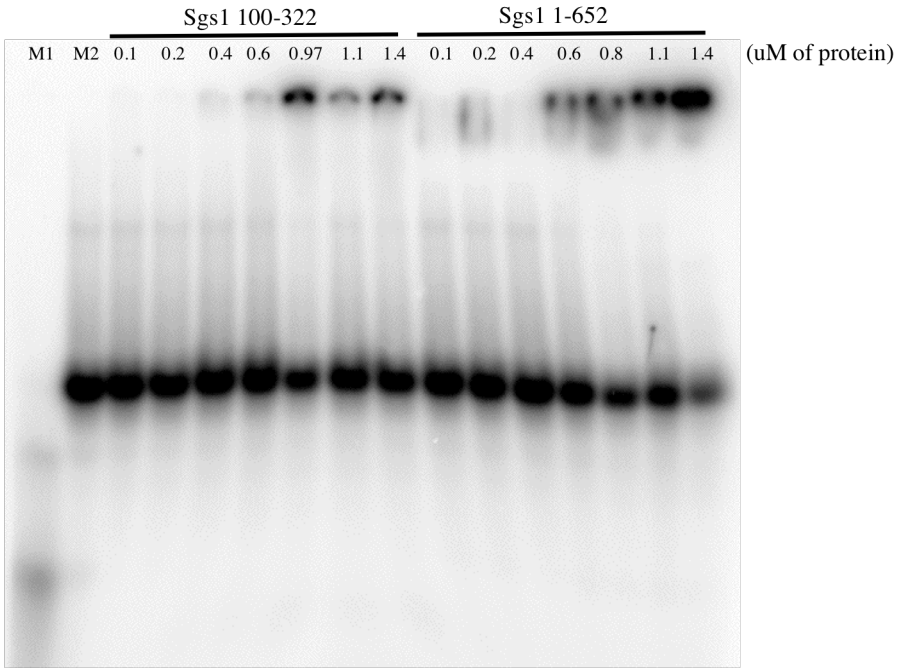

25mM Tris-HCl 7.5, 1mM DTT, BSA 0.1 ug/ul, 10 mM NaCl
Reaction Time: 15 min, Temp 25
[P-32 Holiday Junction 1nM]
M1 - Boiled HJ for 1min - no protein
M2 - HJ alone - no protein

Figure 21. Titration of binding activity of Sgs1$_{1-652}$ and Sgs1 $_{103-323}$ to DNA HJ substrate. *The above GST–Sgs1 fusion proteins were subjected to EMSA assay using ^{32}P-labelled DNA oligo substrate of HJ as a probe. Protein concentration titrated as noted to compare binding ability of the two proteins.*

Perry and colleagues recently identified a coiled coil domain in the RecQ helicase protein of Werner (Perry et al 2010), which led Chen and Brill to consider replacing the SE domain with a coiled coil to see if this would restore complementation in the synthetic lethality assay. They constructed a chimera with the classic example of a coiled coil, the GCN4 leucine zipper (PDB accession code 1zik) using aa 227-281 and found that it did restore complementation (Chen and Brill unpublished data). Running Coils, a program that compares a sequence to a database of known parallel two-stranded coiled-coils and derives a similarity score, a possible coiled coil region can be mapped to Sgs1 aa 227-248 (Fig. 22, 23 and 24) (Lupas et al. 1991).

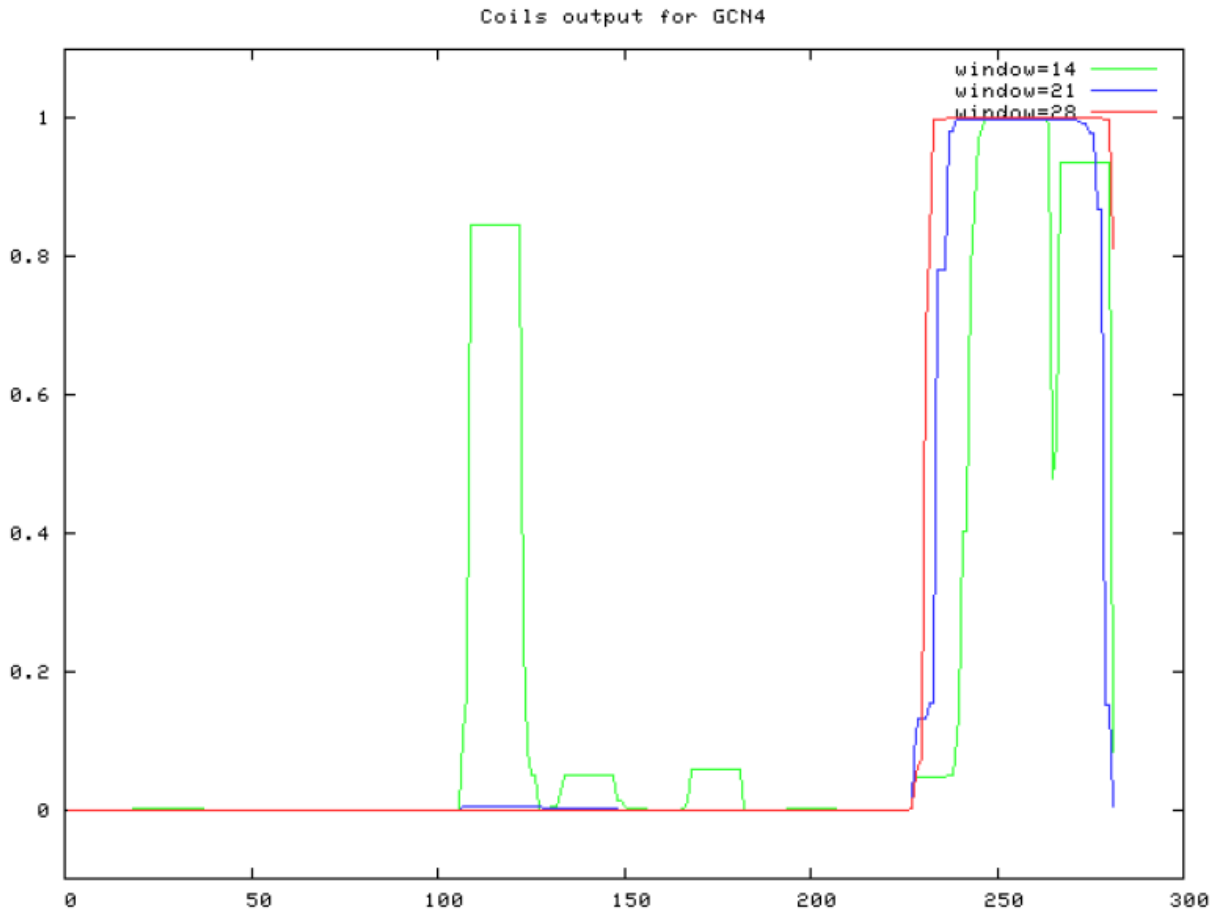

Figure 22. Coils output for GCN4. *Coils program was run with the protein sequence of GCN4 1-281(a classic coiled coil leucine zipper) as an example of an output for a coiled coil region. The default option was used which gives residue number, residue type and the frame and coiled-coil-forming probability obtained in scanning windows of 14, 21 and 28 residues. COILS yields a set of probabilities that presumably reflect the coiled-coil forming potential of a sequence. This means that even at high probabilities (e.g. >90%), there will be (and should be) sequences that in fact do not form a coiled coil, though they may have the potential to do so in a different context. (Lupas et al. 1991). The coiled coil region can be mapped to aa 227-281.*

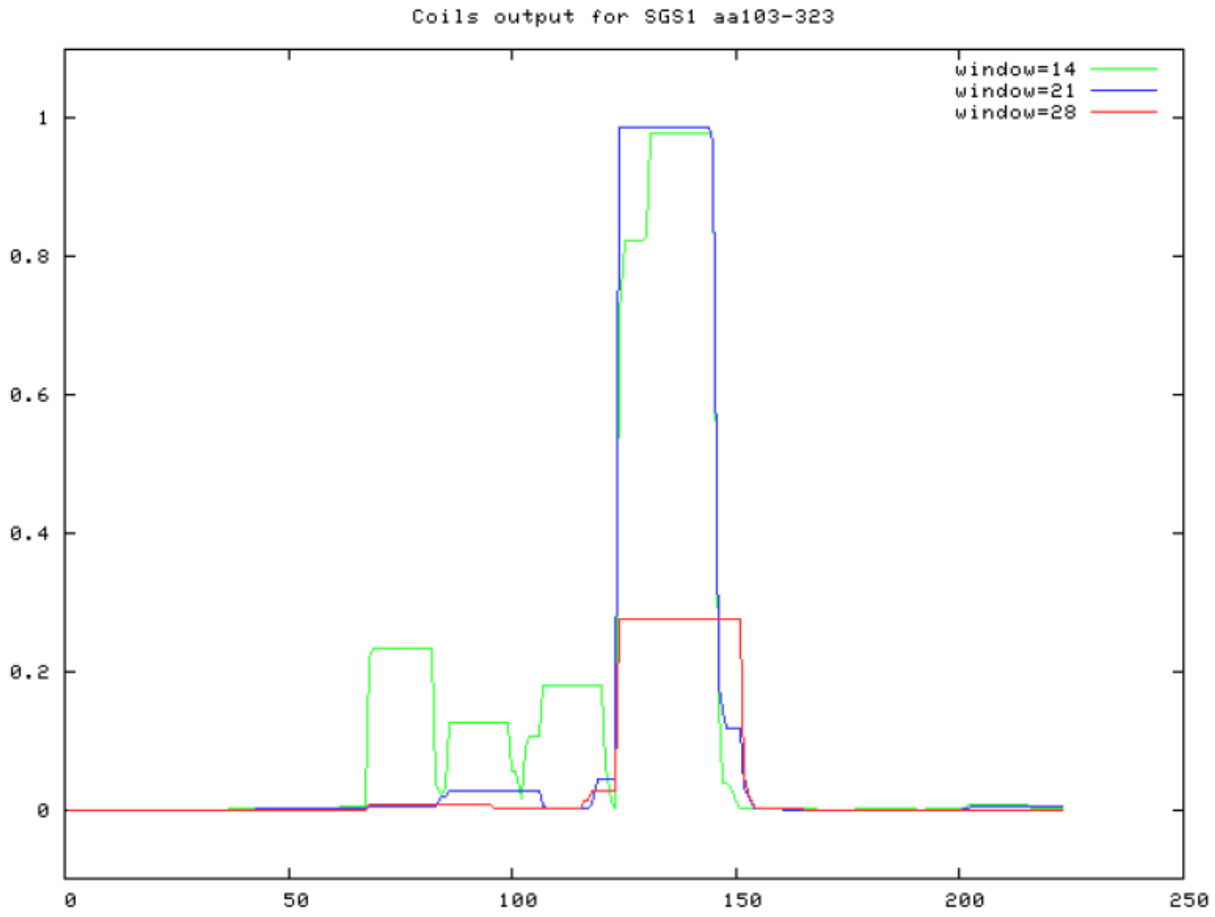

Figure 23. Coils output for SGS1 $_{103\text{-}323.}$ *Coils program was run with the protein sequence of SGS1* $_{103\text{-}323.}$ *To identify any possible coil coiled regions. The default option was used which gives residue number, residue type and the frame and coiled-coil-forming probability obtained in scanning windows of 14, 21 and 28 residues. COILS yields a set of probabilities that presumably reflect the coiled-coil forming potential of a sequence. This means that even at high probabilities (e.g. >90%), there will be (and should be) sequences that in fact do not form a coiled coil, though they may have the potential to do so in a different context. (Lupas et al. 1991). For scanning windows 14 and 21 there is a 100% probability for a coil coiled region and this can approximately be mapped to SGS1* $_{227\text{-}248.}$

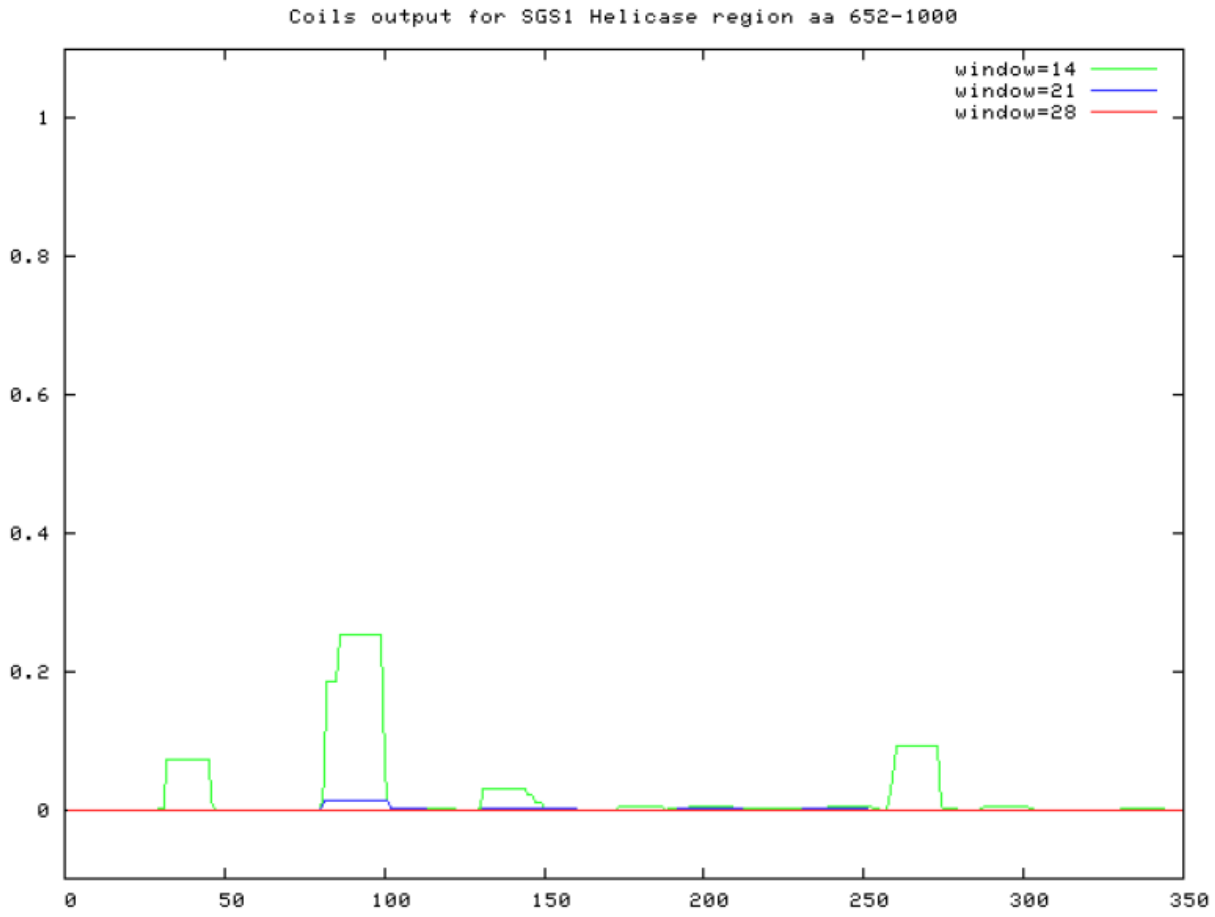

Figure 24. Coils output for SGS1 helicase domain aa 652-1000. *Coils program was run with the protein sequence of SGS1* $_{652\text{-}1000.}$, *to illustrate a negative result for a coil coiled region. The default option was used which gives residue number, residue type and the frame and coiled-coil-forming probability obtained in scanning windows of 14, 21 and 28 residues. COILS yields a set of probabilities that presumably reflect the coiled-coil forming potential of a sequence. This means that even at high probabilities (e.g. >90%), there will be (and should be) sequences that in fact do not form a coiled coil, though they may have the potential to do so in a different context. (Lupas et al. 1991*

In light of the above-unpublished data, we thought it might be fruitful to repeat the internal deletions of Sgs1 in the area of aa 323-652 but with the *GCN4/SGS1* chimera where Sgs1 aa 103-323 was replaced by *GCN4* aa 227-281. The goal was to systematically search for an essential domain, that also required a domain within the SE domain (aa 103-323) that is not involved in its strand exchange functionality (as restored by the insertion of the GCN4 coiled coil domain). This search was completed using the synthetic lethality assay.

All plasmids that were constructed and their results in the *sgs1*Δ *slx4*Δ synthetic lethal assay are listed in the supplemental figures, and are illustrated as deletions from the right side in Fig. 25 and deletions from the left side in Fig. 26. For the deletions from the right side (Fig. 25) the *sgs1/gcn4* chimera alleles behaved exactly the same as the non-chimera alleles and therefore the results are not significant. In Figure 26, however, the non-chimera allele with the deletion of aa 500-621 (p1643) grew (albeit weakly) and in contrast, the *sgs1/gcn4* chimerical allele (p1713) with an identical deletion, did not survive in the *sgs1*Δ *slx4*Δ background. This may prove significant, especially if Bernstein's results are taken into account as their allele of *sgs1*-Δ*502-648* closely approximates our allele of p1643. I would postulate that there may be 2 domains that are dependent upon each other, the AR2 domain and some region within the SE domain.

Furthermore, as we have possibly mapped a coiled coil region to Sgs1 aa 227-281 within the SE domain. It would be interesting to construct an allele with this deletion and evaluate if it has the same phenotype as the SE domain. If it does, then a series of deletion could be constructed in the area of aa 281 to 652, to evaluate the location of an essential domain and subject it to phenotypic assays.

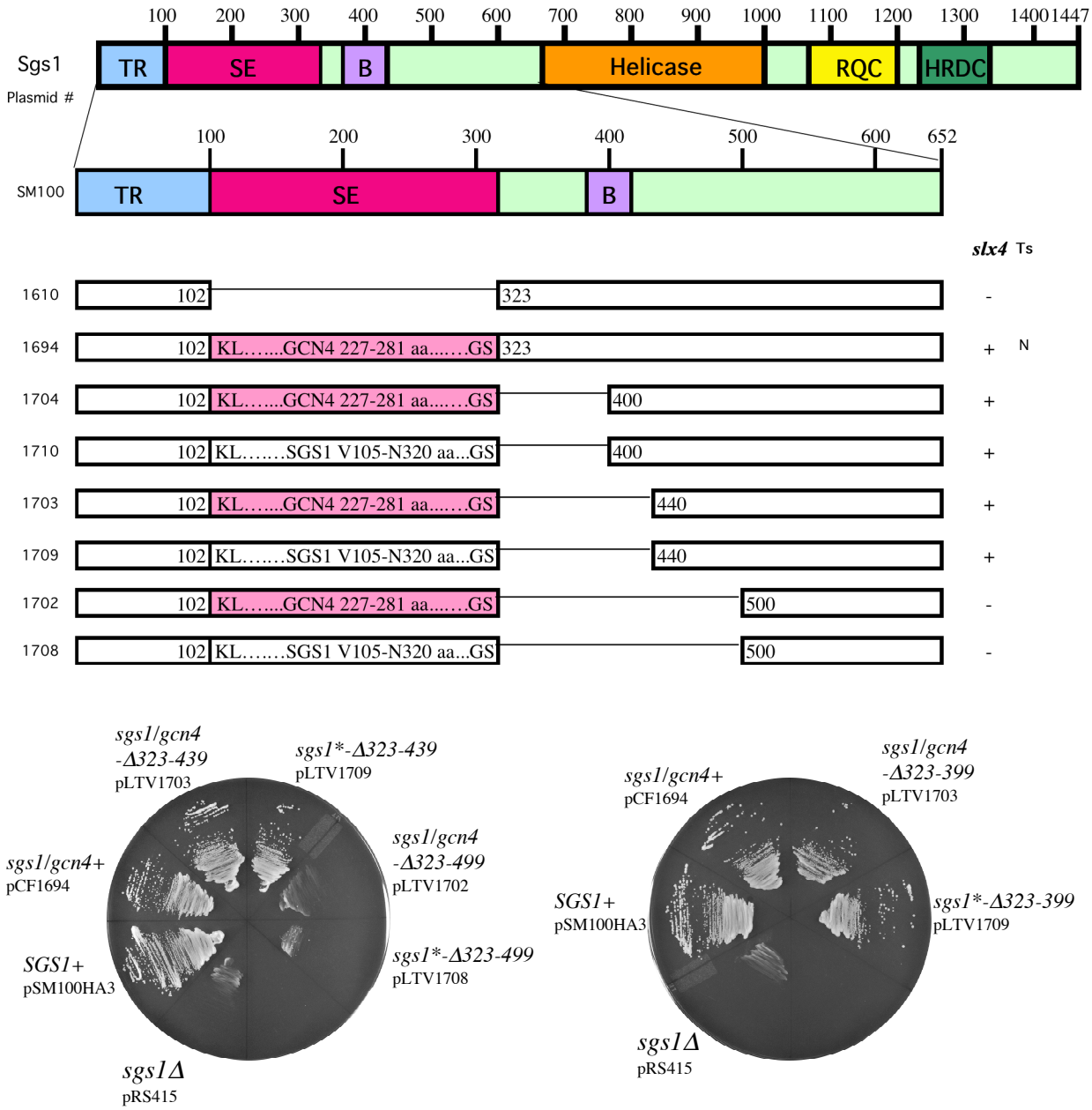

Figure 25. Synthetic lethal assay for plasmids with* SGS1/GCN4 *chimeras. *(a) Schematic alignment of Sgs1 and internal deletions. Sgs1 functional domains:- TR –Top3/Rmi1 binding domain. SE –Strand Exchange. B- putative BDHCT. RQC-RecQ C-terminal. HRDC- RNAseD C-terminal. Plasmid's and aa deletions schematically represented and aa and plasmid #'s noted (b) Strain NJY2083 (sgs1–11::loxP slx4–11::loxP plus pJM500 (SGS1/ URA3/ADE3/CEN) was transformed with various SGS1 alleles in pRS415 as indicated in the key. Transformants were streaked onto plates containing 5-FOA and the plates were photographed after 2 (sgs1Δ slx4Δ) days growth at 30°C*

Figure 26.

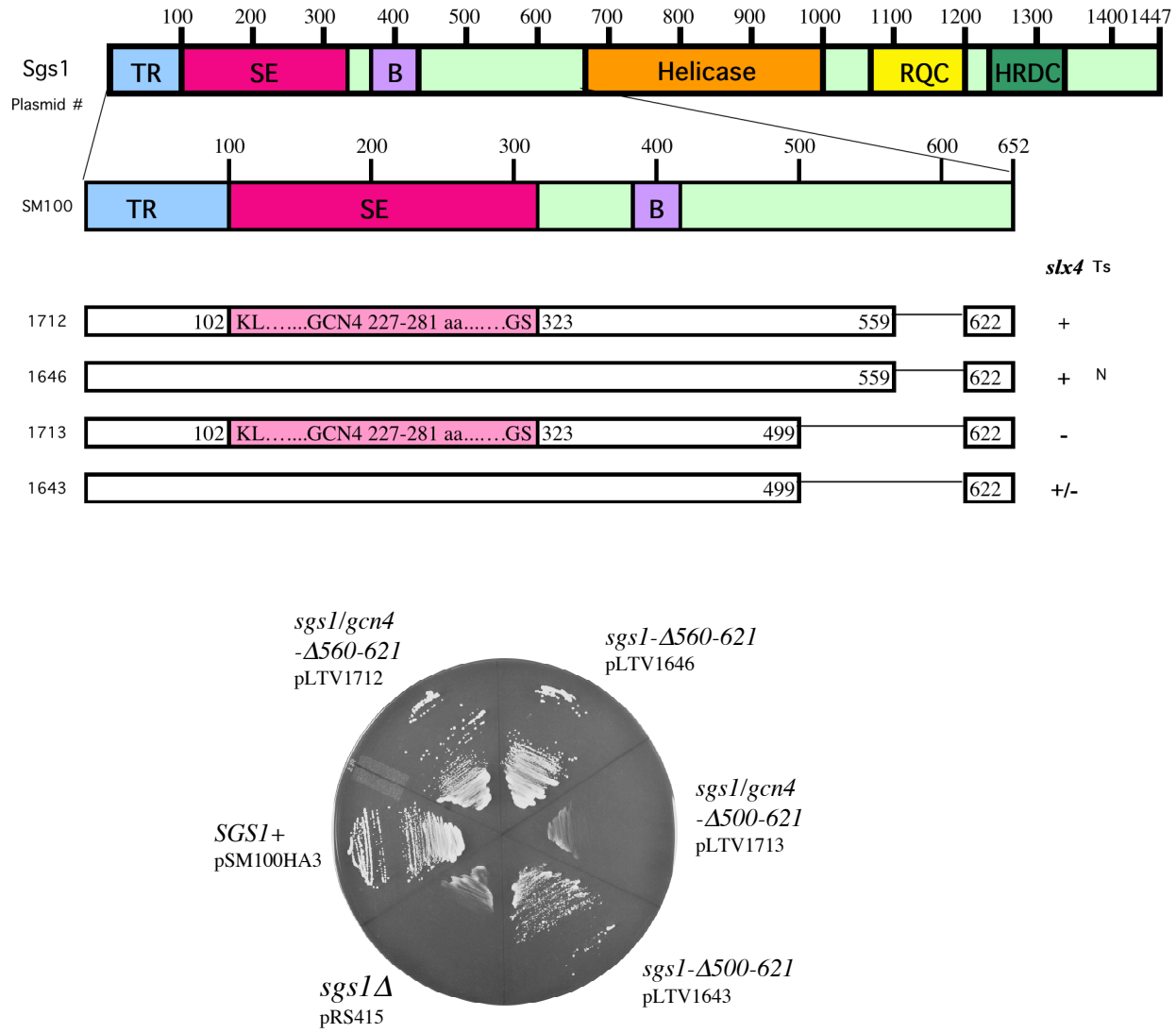

Figure 26. Synthetic lethal assay for plasmids with* SGS1/GCN4 *chimeras. *(a) Schematic alignment of Sgs1 and internal deletions. Sgs1 functional domains:- TR –Top3/Rmi1 binding domain. SE –Strand Exchange. B- putative BDHCT. RQC-RecQ C-terminal. HRDC- RNAseD C-terminal. Plasmid's and aa deletions schematically represented and aa and plasmid #'s noted (b) Strain NJY2083 (sgs1–11::loxP slx4–11::loxP plus pJM500 (SGS1/ URA3/ADE3/CEN) was transformed with various SGS1 alleles in pRS415 as indicated in the key. Transformants were streaked onto plates containing 5-FOA and the plates were photographed after 2 (sgs1Δ slx4Δ) days growth at 30°C*

In conclusion I have found a domain that is important to Sgs1's function through performing structure/function analyses of Sgs1 in its poorly characterized N-terminus of aa 323-652. I interrogated this region by doing systematic deletions and tested these *sgs1* mutants for complementation of synthetic lethality. The allele with the smallest deletion that did not complement *sgs1slx4* synthetic lethality was found to be *sgs1-Δ386-621,* and allele with the smallest deletion that did not complement *sgs1slx5*, was found to be *sgs1-Δ500-621*. I found that *sgs1-Δ386-621* is physiologically important also through the Top3 slow growth assay. Furthermore I believe that the difference in results between *sgs1slx4* and *sgs1slx5* will prove significant and warrants further investigation.

I also used a *BLM/GCN4* chimera where the SE domain was replaced with the coiled coil GCN4, and again tested alleles with systematic deletions within aa 323-652 in synthetic lethality assay. I found the smallest essential domain to be *sgs1/gcn4-Δ500-621* in the *sgs1slx4* background, and interestingly the same deletion in *sgs1-Δ500-621* did grow weakly and complemented synthetic lethality. Therefore I postulate there is some interaction between the SE domain and aa 500-621 (approximately the AR2 aa 502-648 as per Bernstein and colleagues) that could be physiologically important and warrants further investigation.

Experimental Methods

Genetic Assay's

Synthetic lethality, MMS sensitivity and genetic recombination were assayed as described (Mullen et al. 2000).

Construction of Plasmids and for the Mutant alleles.

PCR-mediated gene disruptions were designed to replace complete open reading frames (ORFs) or parts of the gene. Supplemental Figures 1 and 2 is a schematic diagram of plasmids constructed with the residues deleted noted and their results in the synthetic lethal assays. Supplemental Tables 1 and 2 lists all the plasmids constructed, with vectors and the PCR oligonucleotides used to construct the inserts for the PCR-mediated gene disruptions.

Proteins used in EMSA DNA binding assay

All GST-fusion proteins ($Sgs1_{1\text{-}652}$, $Sgs1_{323\text{-}652}$, $Sgs1_{103\text{-}322}$, $Sgs1_{484\text{-}652}$, $Sgs1_{103\text{-}250}$) generously provided by Chi Fu Chen and expressed and purified as per Chen et al. 2010.

EMSA DNA binding assay

^{32}P-labeled DNA substrates were prepared and assayed by EMSA essentially as described (Mullen et al. 2005). Proteins were incubated with ^{32}P-labeled DNA substrate in a final volume of 20 µl containing 25 mM Tris (pH 7.5), 10 mM NaCl, 1 mM dithiothreitol, 0.1 mg/ml BSA, and at 25°C for 15 min. Loading dye was added to a final concentration of 8% glycerol and

0.25% bromophenol blue. Oligonucleotide binding was tested by electrophoresis at 10 volts/cm through a 10% polyacrylamide gel (29:1 acrylamide:bis) in 1X TBE at room temperature. The gel was fixed in 50% EtOH/10% acetic acid for 15 min, dried, and visualized by a Molecular Dynamics phosphorimager.

DNA substrates

The sequences of the oligonucleotide substrates that were taken from (Whitby and Dixon 1998) as follows: branch-migratable Holliday junction, oligos 1253(5'-TGGGTCAACGTGGGCAAAGATGTCCTA GCAATGTAATCGTCTATGACGTT-3'), 1254 (5'-TGCCGAATTCTACCA GTGCCAGTGATGGACATCTTTGCCCACGTTGACCC-3'), 1255 (5'-GTCGGATCCTCTAGACAGCTCCATGATCACTGGCACTGGTAGAATTCGGC-3'), and 1256 (5'-CAACGTCATAGACGATTACATTGCTACATGGAGCTGTCTAGAGGATCCGA-3'). The oligonucleotides (IDT) used for construction of the D-Loop: oligos 2493 (5'-AGCTCCTAGGGTTACAAGCTTCACTAGGGTTGTCCAGTCACAGTCAGAGTCACAGTC CTACACATGTAGGGTTGATCAGC-3'), 2494 (5'-GCTGATCAACCCTACATGTGTAGGTAACCGGATCCCTAACCCTAAGGACAACCCTAG TGAAGCTTGTAACCCTAGGAGCT-3'), 2496 (5'-TTTTTTTTTTTTTTTTTTTTTTAGGGTTAGGGATCCGGTTA-3')

Supplemental Tables and Figures

Supplemental Figure 1.
Plasmids used and synthetic lethality results

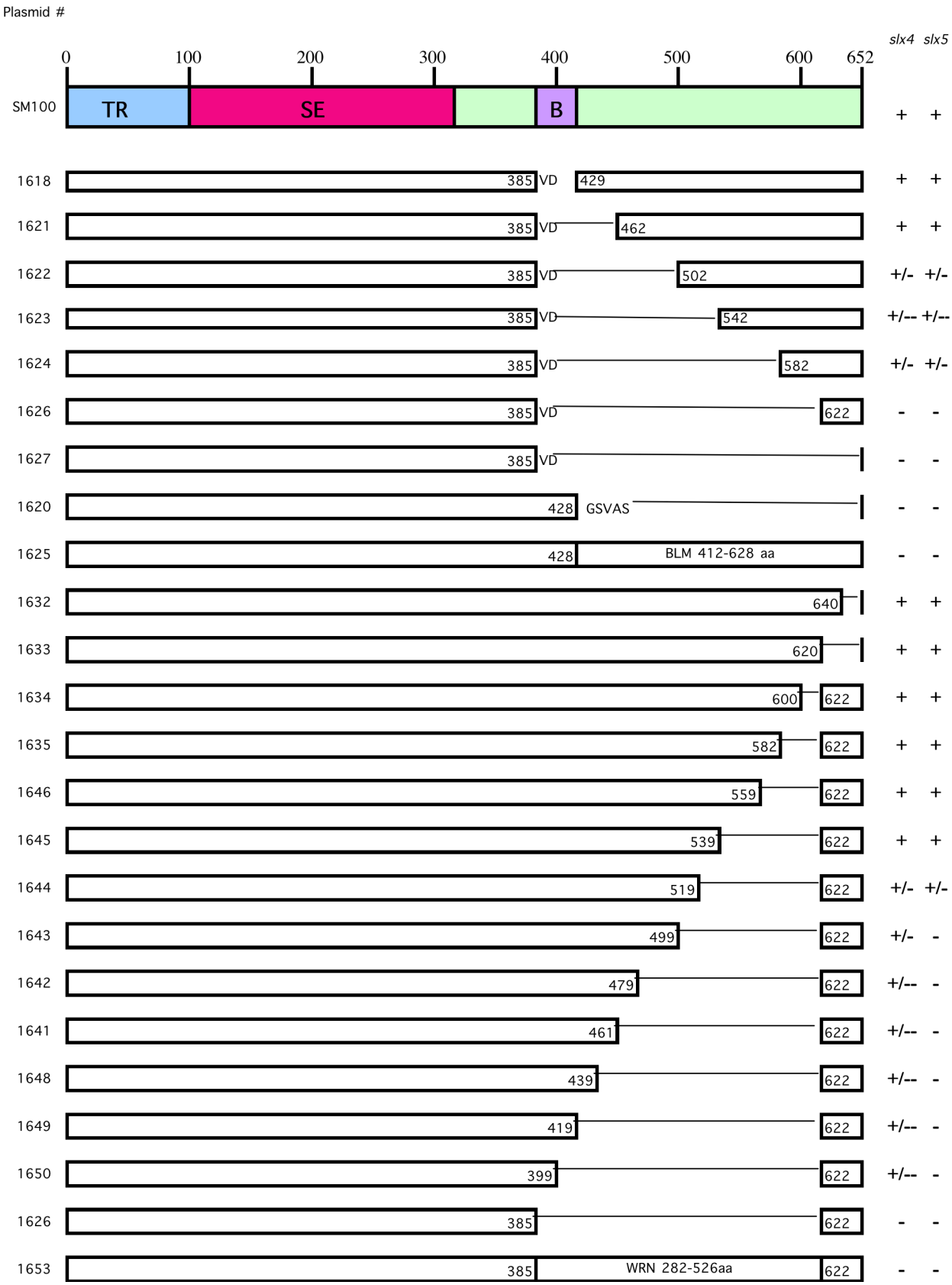

Supplemental Figure 2.
Plasmids used and synthetic lethality results

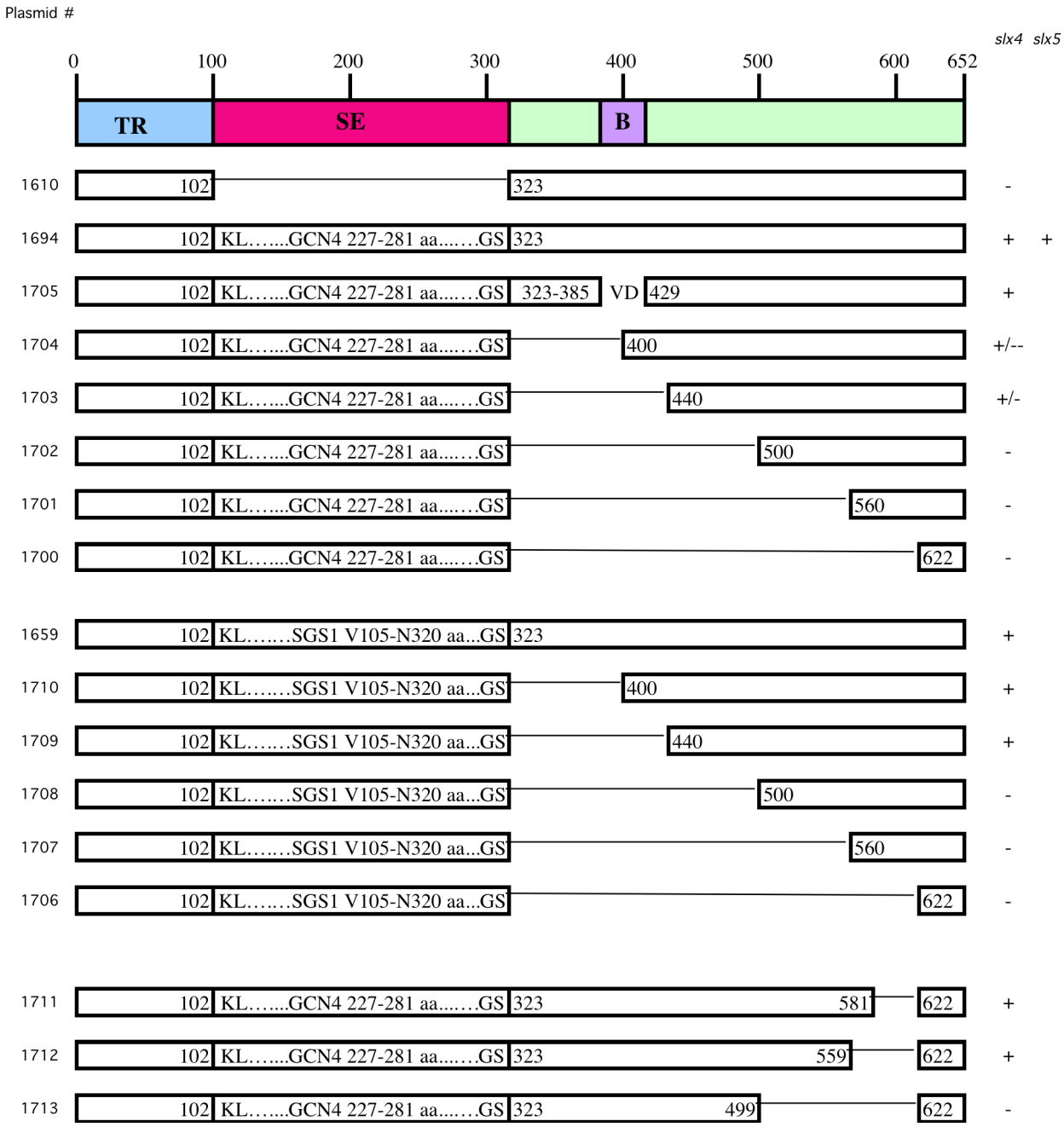

Supplemental Table 1.
Plasmids and oligo's used to construct them

Plasmid #	Approx Plasmid Size bp	Vector #	First Round PCR Forward Oligo	First Round PCR Reverse Oligo	Second Round PCR Forward	Second Round PCR Reverse
1618	10,425	100HA3	316 2613	2614 540	316	540
1620	9,879	100HA3	361 2618	2619 2617	316	2617
1621	10,320	1618	2656	2617		
1622	10,200	1618	2657	2617		
1623	10,086	1618	2658	2617		
1624	9,926	1618	2659	2617		
1625	10,527	1620	2662	2663		
1626	9,843	1618	2664	2617		
1627	9,753	1618	2665	2617		
1632	10,515	100HA3	316 2707	2708 2617	316	2617
1633	10,458	100HA3	316 2709	2710 2617	319	2617
1634	10,488	100HA3	316 2711	2712 2617	316	2617
1635	10,434	100HA3	316 2713	2714 2617	316	2617
1641	10,074	100HA3	316 316	2739 2617	316	2617
1642	10,128	100HA3	316 2740	2741 2617	316	2617
1643	10,188	100HA3	316 2742	2743 2617	316	2617
1644	10,251	100HA3	316 2744	2745 2617	316	2617
1645	10,308	100HA3	316 2746	2747 2617	316	2617
1646	10,368	100HA3	316 2748	2749 2617	316	2617
1648	10,008	100HA3	316 2787	2788 2617	316	2617
1649	9,948	100HA3	316 2789	2790 2617	316	2617
1650	9,888	100HA3	316 2791	2792 2617	316	2617
1653	10,575	1618	2888 2889	2890 2617	2888	2617

Supplemental Table 2.
Plasmids and oligo's used to construct them

Plasmid #	Approx Plasmid Size bp	Vector #	First Round PCR Forward Oligo	First Round PCR Reverse Oligo	Second Round PCR Forward Oligo	Second Round PCR Reverse Oligo
1700	8,975	1694	2909	498		
1701	9,161	1694	2910	498		
1702	9,341	1694	2911	498		
1703	9,521	1694	2912	498		
1704	9,641	1694	2913	498		
1705	9,746	1694	2914	498		
1706	9,475	1659	2909	498		
1707	9,661	1659	2910	498		
1708	9,841	1659	2911	498		
1709	10,021	1659	2912	498		
1710	10,141	1659	2913	498		
1711	9,925	1694	2537 2713	2714 498	2537	498
1712	9,859	1694	2637 2748	2749 498	2537	498
1713	9,679	1694	2537 2742	2743 498	2537	498

References

1. Amin AD, Chaix ABH, Mason RP, Badge RM, Borts RH (2010) The Roles of the Saccharomyces cerevisiae RecQ Helicase SGS1 in Meiotic Genome Surveillance. PLoS ONE 5(11): e15380. doi:10.1371/journal.pone.0015380
2. Ashton TM. Hickson ID. (2010) Yeast as a model system to study RecQ helicase function. DNA Repair. 9(3):303-14
3. Bahr, A., F. De Graeve, et al. (1998). "Point mutations causing Bloom's syndrome abolish ATPase and DNA helicases activities of the BLM protein." Oncogene 17(20): 2565-71.
4. Bennett RJ, Keck J, Wang J. (1999). Binding specificity determines polarity of DNA unwinding by the Sgs1 protein of S. cerevisiae. J. Mol. Biol. 289:235–48
5. Bennett, R. J. & Keck, J. L. (2004) Structure and function of RecQ DNA helicases. Crit. Rev. Biochem. Mol. Biol. 39, 79–97
6. ennett, RJ and Wang JC (2001) Association of yeast DNA topoisomerase III and Sgs1 DNA helicase: studies of fusion proteins. Proc Natl Acad Sci U S A 98(20): 11108-13.
7. Bernstein KA, Gangloff S, Rothstein RR (2010). The RecQ DNA Helicases in DNA Repair. Annual Review of Genetics Vol. 44: 393-417
8. Bernstein KA, Rothstein R, (2009) At loose ends: resecting a double-strand break, Cell 137 807–810.
9. Bernstein KA, Shor E, Sunjevaric I, Fumasoni M, Burgess RC, et al. (2009) Sgs1 function in the repair of DNA replication intermediates is separable from its role in homologous recombinational repair. EMBO J. 28:915–25
10. Bjergbaek L, Cobb JA, Tsai-Pflugfelder M, Gasser SM (2005), Mechanistically distinct roles for Sgs1p in checkpoint activation and replication fork main- tenance, EMBO J. 24 405–417.
11. Bussen W, Raynard S, Busygina V, Singh AK Sung P. (2007) Holliday junction processing activity of the BLM–TopoIIIalpha–BLAP75 complex. J. Biol. Chem. 282, 31484–31492.
12. Cejka P, Kowalczykowski SC. (2010). The full-length Saccharomyces cerevisiae Sgs1 protein is a vigorous DNA helicase that preferentially unwinds Holliday junctions. J. Biol. Chem. 285:8290–301
13. Cejka P. Cannavo E, Polaczek P, Masuda-Sasa T, Pokharel S, Campbell J, Kowalczykowski SC. (2010) DNA end resection by Dna2-Sgs1-RPA and its stimulation by Top3-Rmi1 and Mre11-Rad50-Xrs2. Nature Vol 467 p112-117
14. Cesare AJ, Reddel RR, (2008) Telomere uncapping and alternative lengthening of telomeres, Mech. Ageing Dev. 129 99–108
15. Chakraverty RK, Kearsey JM, Oakley TJ, Grenon M, de La Torre Ruiz MA, Lowndes NF, Hickson ID (2001) Topoisomerase III acts upstream of Rad53p in the S-phase DNA damage checkpoint, Mol. Cell. Biol. 21 (2001) 7150– 7162.

16. Chang, M., Bellaoui M, Zhang C, Desai R, Morozov P, Delgado-Cruzata L, Rothstein R, Freyer GA, Boone C, Brown GW (2005) RMI1/NCE4, a suppressor of genome instability, encodes a member of the RecQ helicase/Topo III complex. EMBO J. 24, 2024–2033
17. Chen CF, Brill SJ. (2010) An essential DNA strand-exchange activity is conserved in the divergent N-termini of BLM orthologs. EMBO J. 29:1713–25
18. Chen, C. F. and S. J. Brill (2007). "Binding and activation of DNA topoisomerase III by the Rmi1 subunit." J Biol Chem 282(39): 28971-9.
19. Chu WK, Hickson ID (2009. “RecQ helicases: multifunctional genome caretakers” Nat Rev Cancer. :644-54
20. Chiolo I et al. (2005) Srs2 and Sgs1 DNA helicases associate with Mre11 in different subcomplexes following checkpoint activation and CDK1-mediated Srs2 phosphorylation. Mol. Cell. Biol. 25, 5738–5751
21. Cobb JA, Bjergbaek L, Shimada K, Frei C, Gasser SM. (2003) DNA polymerase stabilization at stalled replication forks requires Mec1 and the RecQ helicase Sgs1. EMBO J. 22:4325–36
22. Dunderdale HJ, Benson FE, Parsons CA, Sharples GJ, Lloyd RG, West SC (1991) Formation and resolution of recombination intermediates by E. coli RecA and RuvC proteins, Nature 354 506–510.
23. Erzberger JP, Berger JM. (2006) Evolutionary Relationships and Structural Mechanisms of AAA+ Proteins Annu. Rev. Biophys. Biomol. Struct. 35:93–114
24. Finn RD, Mistry J, Tate J, Coggill, Heger A, Pollington JE, Gavin OL, Gunesekaran P, Ceric G, Forslund K, Holm L, Sonnhammer EL, Eddy SR, Bateman A. The Pfam protein families database (2010) Nucleic Acids Research Database Issue 38:D211-222
25. Frei C, Gasser SM (2000) The yeast Sgs1p helicase acts upstream of Rad53p in the DNA replication checkpoint and colocalizes with Rad53p in S-phase-specific foci, Genes Dev. 14 (2000) 81–96.
26. Fricke WM, Brill SJ (2003) Slx1–Slx4 is a second structure-specific endonuclease functionally redundant with Sgs1–Top3, Genes Dev. 17 1768–1778.
27. Fricke WM, Kaliraman V, Brill SJ, (2001) Mapping the DNA topoisomeraseIII binding domain of the Sgs1 DNA helicase, J. Biol. Chem. 276 (2001) 8848–8855.
28. Gangloff S, de Massy B, et al. (1999) The essential role of yeast topoisomerase III in meiosis depends on recombination EMBO J 18(6): 1701-11.
29. Gangloff S, McDonald JP, Bendixen C, Arthur L, Rothstein R. (1994) The yeast typeI topoisomerase Top3 interacts with Sgs1, a DNA helicase homolog: a potential eukaryotic reverse gyrase. Mol. Cell. Biol. 14, 8391–8398
30. Harmon F, Kowalczykowski S. (1998). RecQ helicase, in concert with RecA and SSB proteins, initiates and disrupts DNA recombination. Genes Dev. 12:1134–44
31. Heyer WD, Ehmsen KT, Solinger JA, (2003) Holliday junctions in the eukaryotic nucleus: resolution in sight? Trends Biochem. Sci. 28, 548–557
32. Hickman ID, Burgess A, Dyda F. (2005) Binding and unwinding: SF3 viral helicases. Current Opinion in Structural Biology, Feb2005, Vol. 15 Issue 1, p77-85, 9p

33. Huang P, Pryde FE, Lester D, Maddison RL, Borts RH, Hickson ID, Louis EJ (2001) SGS1 is required for telomere elongation in the absence of telomerase. Curr. Biol. 11, 125–129
34. Huang S, Lee L, Hanson NB, Lenaerts C, Hoehn H, et al. (2006) The spectrum of WRN mutations in Werner syndrome patients. Hum. Mutat. 27:558–67
35. Huber MD, Duquette M L, Shiels J C, Maizels N. (2006). A conserved G4 DNA binding domain in RecQ family helicases. J. Mol. Biol. 358, 1071–1080.
36. Ip SC, Rass U, Blanco MG, Flynn HR, Skehel JM, West SC (2008) Identification of Holliday junction resolvases from humans and yeast, Nature 456 357–361.
37. Ira G, Malkova A, Liberi G, Foiani M Haber JE (2003) Srs2 and Sgs1–Top3 suppress crossovers during double-strand break repair in yeast. Cell 115, 401–411
38. Kaplan DL, O'Donnell M. (2002) DnaB drives DNA branch migration and dislodges proteins while encircling two DNA strands. Molecular Cell.S Vol. 10, Issue 3, p647-657, 11p
39. Lee J W, Harrigan J, Opresko PL, Bohr VA (2005) Pathways and functions of the Werner syndrome protein. Mech. Ageing Dev. 126, 79–86
40. Liberi G, Maffioletti G, Lucca C, Chiolo I, Baryshnikova A, Cotta-Ramusino C, Lopes M, Pellicioli A, Haber JE, Foiani M, (2005) Rad51-dependent DNA structures accumulate at damaged replication forks in sgs1 mutants defective in the yeast ortholog of BLM RecQ helicase, Genes Dev. 19 339–350.
41. Lupas, A., Van Dyke, M., and Stock, J. (1991) Predicting Coled Coils from Protein Sequences,Science 252:1162-1164
42. Mankouri HW, Hickson ID (2003) Top3 processes recombination intermediates and modulates checkpoint activity after DNA damage, Mol. Biol. Cell. 17 (2006) 4473–4483.
43. Mankouri HW, Hickson ID, (2007) The RecQ helicase-topoisomerase III-Rmi1 complex: a DNA structure-specific 'dissolvasome'? Trends Biochem. Sci. 32 538–546.
44. Mankouri HW, Ngo HP, Hickson ID (2007) Investigating the role(s) of the Sgs1–Top3–Rmi1 complex in homologous recombination repair in S. cere- visiae, Mutagenesis 22 448–1448.
45. Mirzaei H, Syed S, Kennedy J, Schmidt KH. (2011) Sgs1 truncations induce genome rearrangements but suppress detrimental effects of BLM overexpression in Saccharomyces cerevisiae. J Mol Biol. 2011 Jan 28;405(4):877-91
46. Miyajima A, Seki M, Onoda F, Ui A, Satoh Y, Ohno Y, Enomoto T. (2000) Different domains of Sgs1 are required for mitotic and meiotic functions. Genes Genet. Syst. 75, 319–326.
47. Mohaghegh P, Karow JK, Brosh RM Jr, Bohr VA, Hickson ID. (2001). The Bloom's and Werner's syndrome proteins are DNA structure-specific helicases. Nucleic Acids Res. 29:2843–49
48. Mullen JR, Nallaseth FS, Lan YQ, Slagle CE, Brill SJ, (2005) YeastRmi1/Nce4 controls genome stability as a subunit of the Sgs1–Top3 complex, Mol. Cell. Biol. 25 4476–4487.
49. Mullen JR, Kaliraman V, et al. (2000) Bipartite structure of the SGS1 DNA helicase in Saccharomyces cerevisiae. Genetics 154: 1101-14.

50. Mullen JR, Chen CF, Brill SJ. (2010) Wss1 Is a SUMO-Dependent Isopeptidase That Interacts Genetically with the slx5-slx8 SUMO-Targeted Ubiquitin Ligase. Molecular & Cellular Biology. 30(15):3737-48

51. Myung K, Datta A, Chen C, Kolodner RD (2001). SGS1, the Saccharomyces cerevisiae homologue of BLM and WRN, suppresses genome instability and homeologous recombination. Nat Genet 27(1): 113-6.
52. Niu H, Chung W, Zhu Z, Kwon Y, Zhao W, Chi P, Prakash R, Seong C, Liu D, Lu L, Ira G, Sung P. (2010) Mechanism of the ATP-dependent DNA end- resection machinery from Saccharomyces cerevisiae. Nature Vol 467 p112-117
53. Oh SD, Lao JP, Hwang PY-H, Taylor AF, Smith GR, et al. (2007) BLM Ortholog, Sgs1, Prevents Aberrant Crossing-over by Suppressing Formation of Multichromatid Joint Molecules. Cell 130: 259–272.
54. Osman F, Whitby MC (2007) Exploring the roles of Mus81–Eme1/Mms4 at per- turbed replication forks, DNA Repair (Amst.) 6 1004–1017.
55. Patel SS, Picha KM, (2000) Structure and function of hexameric helicases. Annual Review of Biochemistry. 69:651-97,
56. Perry JJ, Asaithamby A, Barnebey A, Kiamanesch F, Chen DJ, Han S, Tainer JA, Yannone SM. (2010) Identification of a coiled coil in werner syndrome protein that facilitates multimerization and promotes exonuclease processivity. J Biol Chem. 13;285(33):25699-707
57. Plank, J.L. & Hsieh, T.S. (2006) A novel, topologically constrained DNA molecule containing a double Holliday junction: design, synthesis, and initial biochemical characterization. J. Biol. Chem. 281, 17510–17516.
58. Plank, J.L., Wu, J. & Hsieh, T.S. (2006). Topoisomerase III alpha and Bloom's helicase can resolve a mobile double Holliday junction substrate through convergent branch migration. Proc. Natl. Acad. Sci. USA 103, 11118–11123
59. Raynard, S. et al. (2008) Functional role of BLAP75 in BLM–topoisomerase IIIalpha-dependent Holliday junction processing. J. Biol. Chem. 283, 15701–15708.
60. Raynard, S., Bussen, W. & Sung, P. (2006) A double Holliday junction dissolvasome comprising BLM, topoisomerase IIIalpha, and BLAP75. J. Biol. Chem. 281, 13861–13864.
61. Seki M, Otsuki M, Ishii Y, Tada S, Enomoto T. (2008). RecQ family helicases in genome stability. Cell Cycle 7:2472–78
62. Singleton MR, Dillingham MS, Wigley DB, (2007) Structure and mechanism of helicases and nucleic acid translocases. Annual Review of Biochemistry. 76:23-50
63. Sugawara N, Goldfarb T, Studamire B, Alani E, Haber JE, (2004) Heteroduplex rejection during single-strand annealing requires Sgs1 helicase and mismatch repair proteins Msh2 and Msh6 but not Pms1, Proc. Natl. Acad. Sci. U.S.A. 101 9315–9320.
64. Sun H, Bennett RJ, Maizels N. (1999). The Saccharomyces cerevisiae Sgs1 helicase efficiently unwinds G-G paired DNAs. Nucleic Acids Res. 27:1978–84
65. Svendsen JM, Harper JW. (2010) GEN1/Yen1 and the SLX4 complex: solutions to the problem of Holiday Juction resolution. Genes & Development. 24(6):521-36

66. Ui, A., M. Seki, et al. (2005). "The ability of Sgs1 to interact with DNA topoisomerase III is essential for damage-induced recombination." DNA Repair (Amst) 4(2): 191-201.
67. Van Brabant AJ, Ye T, Sanz M, German IJ, Ellis NA, Holloman WK. (2000). Binding and melting of D-loops by the Bloom syndrome helicase. Biochemistry 39:14617–25
68. von Kobbe C, Thoma NH, Czyzewski BK, Pavletich N P, Bohr VA (2003). Werner syndrome protein contains three structure-specific DNA binding domains. J. Biol. Chem. 278, 52997–53006.
69. Wang, J.C. (2002) Cellular roles of DNA topoisomerases: a molecular perspective. Nat. Rev. Mol. Cell Biol. 3, 430–440.
70. Wu L, Chan K L, Ralf C, Bernstein D A, Garcia PL, Bohr VA. et al. (2005). The HRDC domain of BLM is required for the dissolution of double Holliday junctions. EMBO J. 24, 2679–2687.
71. Wu L, Davies SL,. North PS, Goulaouic H, Riou JF, Turley H, Gatter KC, Hickson ID, (2000) The Bloom's syndrome gene product interacts with topoisomerase III, J. Biol. Chem. 275 9636–9644.
72. Wu L, Hickson ID, (2003) The Bloom's syndrome helicase suppresses crossing over during homologous recombination, Nature 426 (2003) 870–874.
73. Wu, L. et al. (2006) BLAP75/RMI1 promotes the BLM-dependent dissolution of homologous recombination intermediates. Proc. Natl. Acad. Sci. USA 103, 4068–4073.